

UC Berkeley

UC Berkeley Electronic Theses and Dissertations

Title

Improving Energy Efficiency in CNC Machining

Permalink

<https://escholarship.org/uc/item/80t8k1qj>

Author

Pavanaskar, Sushrut S.

Publication Date

2014

Peer reviewed|Thesis/dissertation

Improving Energy Efficiency in CNC Machining

By

Sushrut S. Pavanaskar

A dissertation submitted in partial satisfaction of the

requirements for the degree of

Doctor of Philosophy

in

Engineering - Mechanical Engineering

in the

Graduate Division

of the

University of California, Berkeley

Committee in charge:

Professor Sara McMains, Chair
Professor Carlo Séquin
Professor Alice Agogino

Spring 2014

Improving Energy Efficiency in CNC Machining

Copyright 2014
by
Sushrut S. Pavanaskar

Abstract

Improving Energy Efficiency in CNC Machining

by

Sushrut S. Pavanaskar

Doctor of Philosophy in Engineering - Mechanical Engineering

University of California, Berkeley

Professor Sara McMains, Chair

We present our work on analyzing and improving the energy efficiency of multi-axis CNC milling process.

Due to the differences in energy consumption behavior, we treat 3- and 5-axis CNC machines separately in our work. For 3-axis CNC machines, we first propose an energy model that estimates the energy requirement for machining a component on a specified 3-axis CNC milling machine. Our model makes machine-specific predictions of energy requirements while also considering the geometric aspects of the machining toolpath. Our model and the associated software tool facilitate direct comparison of various alternative toolpath strategies based on their energy-consumption performance.

Further, we identify key factors in toolpath planning that affect energy consumption in CNC machining. We then use this knowledge to propose and demonstrate a novel toolpath planning strategy that may be used to generate new toolpaths that are inherently energy-efficient, inspired by research on digital micrography – a form of computational art. For 5-axis CNC machines, the process planning problem consists of several sub-problems that researchers have traditionally solved separately to obtain an approximate solution. After illustrating the need to solve all sub-problems simultaneously for a truly optimal solution, we propose a unified formulation based on configuration space theory. We apply our formulation to solve a problem variant that retains key characteristics of the full problem but has lower dimensionality, allowing visualization in 2D. Given the complexity of the full 5-axis toolpath planning problem, our unified formulation represents an important step towards obtaining a truly optimal solution.

With this work on the two types of CNC machines, we demonstrate that without changing the current infrastructure or business practices, machine-specific, geometry-based, customized toolpath planning can save energy in CNC machining.

To my parents, Sushama and Shrikant Pavanaskar.

Contents

List of Figures	iv
List of Tables	vi
Acknowledgments	vii
1 Introduction	1
1.1 Research Motivation	1
1.2 CNC Milling and Energy Consumption	2
1.3 Research Outline	3
2 Background and Related Work	5
2.1 Preliminaries	5
2.2 Energy consumption in CNC machines	5
2.3 Analysis and modeling of the 3-axis milling process	7
2.4 Toolpath planning for 5-axis machines	8
2.4.1 Interdependence of sub-problems	10
2.5 Summary	10
3 Modeling Energy Consumption in 3-axis Milling	12
3.1 Past work on modeling CNC milling	12
3.2 Our Proposed Model	15
3.2.1 Determination of customization constants	18
4 Energy Model Applications	24
4.1 Background	24
4.2 Energy analyzer software	25
4.2.1 Software Design	25
4.3 Energy analyzer process flow	26
4.3.1 Software implementation and interface	28
4.4 Validation of energy analyzer predictions	29
4.4.1 Validation of various power states	31
4.4.2 Validation of complete NC codes (toolpaths)	31

4.5	Conclusion	33
5	Energy Analyzer: Examples	34
5.1	Case study 1: Facing operation alternatives	34
5.2	Case study 2: Effect of “corners” in toolpath	36
5.3	Case study 3: Effect of input geometry	39
5.4	Energy analyzer limitations	41
5.5	Summary	42
6	Toward Energy Efficient Toolpaths	43
6.1	Factors Affecting Energy Consumption	43
6.2	Digital micrography	45
6.3	Towards inherently energy efficient toolpaths	47
6.3.1	Setup and toolpath generation	48
6.3.2	Results	50
6.4	Summary	51
7	Toolpath planning for efficiency in 5-axis CNC machining	52
7.1	Introduction	52
7.2	Past work	53
7.2.1	Beyond independent sub-problem solutions	53
7.3	Unified formulation	54
7.3.1	C-space based problem formulation	54
7.3.2	Optimization search	55
7.4	Example implementation	56
7.5	Results and discussion	61
7.5.1	Experimental setup	61
7.5.2	Results: lower dimensional problem	61
7.6	Summary	63
8	Conclusions and Future Work	64
8.1	Future work on 3-axis machining	66
8.2	Future work on 5-axis machining	66
	Bibliography	69

List of Figures

1.1	Energy consumption profiles of three different CNC machines. (Data from [Kordonowy 2002])	2
2.1	Power drawn by a CNC machine as a function of time (symbolic) (a) 3-axis machine, (b) 5-axis machine.	6
2.2	Cutter location (CL), cutter contact (CC), toolpath and scallop in point milling of a freeform surface	8
3.1	Computation of t_{block}	16
3.2	Typical power against time curve for a machining operation with six linear cuts indicating the starting peak/spike in power consumption when the spindle is started.	20
3.3	Typical power against time curve for a machining operation with a single linear demonstrating both, spindle and axis motor spike.	20
3.4	(A) Three superimposed plot of power values against time, recorded by a Yokogawa CW240 on a Haas VF-0 CNC milling machine. (B) Fitting a line to the moving averages of the power values.	22
4.1	Flow-chart for the energy analyzer software	27
4.2	Face-milling a rectangular face	28
4.3	Generating and verifying toolpath for a facing operation in MasterCAM	29
4.4	User interface for providing toolpath parameters after uploading an NC code	30
4.5	The output screen showing the expected time, energy consumption, GHG emissions, and block-by-block plots	31
4.6	(a-f) Schematics of the six toolpaths used in validation checks.	32
5.1	Face-milling a square face with cutting primarily in (a) X-axis direction (b) Y-axis direction	36
5.2	Axes mounting in Haas VF-0 indicating X-axis being mounted atop Y-axis	37
5.3	An industrial CNC machine used in the automotive industry — the Heynumill 3200 PF	38
5.4	(a) Contour-parallel (b) Spiral toolpath for a square facing operation	39
5.5	(a) Contour-parallel (b) Spiral toolpath for a facing operation for a face with islands	40

6.1	Examples of micrographic text arrangements as reported in [Maharik et al. 2011]	45
6.2	(a) Starting 2D geometry, (b) boundary conditions for a desired vector field, (c) a suitable vector field that satisfies the set boundary conditions, (d) tracing vector-field streamlines, orienting and ordering them, and (e) placing text along the streamlines. [Maharik et al. 2011]	46
6.3	Starting 2D geometry	48
6.4	6 alternative strategies from MasterCAM (A) Constant overlap spiral (B) One-way, X-parallel (C) Parallel spiral (D) One-way, Y-parallel (E) True spiral (F) High-speed machining	49
6.5	Schematic toolpaths for the bear component: (left) using direction-parallel strategy in MasterCAM and (right) streamlines generated in digital micrography research that were connected and used as a toolpath. For connecting, Sushrut Pande developed and implemented an algorithm that is reported in [Pande et al. 2013].	49
6.6	Schematic toolpaths for the bear component: (left) using direction-parallel strategy in MasterCAM and (right) using the streamlines generated in digital micrography research.	50
7.1	Lower dimensional problem setup: (a) design curve and cutter; (b) range of possible cutter orientations; (c) scallop height; (d) resulting surface after “machining.”	56
7.2	Solving the lower-dimensional variant. (a) The design curve to be machined and its Bezier control points. (b) Evaluated design curve points. (c) Computed CL path. (d) Concave and convex regions of the design curve. (e) Feasible C-space left after removing global gouging obstacles. (f) Feasible C-space left after removing rear gouging obstacles. (g) Common feasible C-space (intersection of (e) and (f)).	58
7.3	Computing rear and global gouging obstacles (orientation limits)	60
7.4	Results obtained after optimization (a) With equal weights to machining time and MRR (b) With less importance to MRR and more importance to machining time	62

List of Tables

2.1	Past work on 5-axis machining of freeform surfaces	11
4.1	Validation of power states	32
4.2	Validation of NC codes (toolpaths)	32
5.1	Comparison of estimates for facing operation alternatives	35
5.2	Comparison of estimates for spiral and contour parallel toolpaths	39
5.3	Comparison of estimates for spiral and contour parallel toolpaths for a face with islands	41
6.1	Comparison of MasterCAM’s time estimates for the 6 toolpath alternatives. . .	48
6.2	Comparison of time and energy estimates by our energy analyzer with the measured values for the “bear” component.	50

Acknowledgments

At the end of my graduate studies at UC Berkeley, I thank my family, friends, house-mates, and all previous teachers who encouraged, helped, guided, scolded, or prided in me.

I thank Professor Sanjay Pande of IIT Bombay for his valuable guidance through my M. Tech. that helped me get accepted to the graduate program at UC Berkeley. In UC Berkeley, Adarsh Krishnamurthy, Wei Li, and Yusuke Yasui helped me adjust to the new environment; I am grateful for their help. I also thank Peter Cottle, Youngwook Kwon, and Zhongyin Hu for providing valuable feedback on various occasions as my lab-mates.

I am grateful to collaborators: Professor Alla Sheffer from UBC for providing us data from their micrography research, Dr. Wolfgang Bloehs from Audi for his cooperation on the energy analyzer research, Moneer Helu for his help with energy measurements, Anthony Bailey Jr. for his help in the model validation, and Dennis Lee and Gordon Long from the ME student machine shop for their help in conducting machining trials.

Pat Giddings, Donna Craig, Shareena Samson, Yawo Akpawu, and Maria Isabel Blanco supported me in the Mechanical Engineering Department in various administrative and supportive roles; I thank them for their service.

I thank my qualifying exam committee of Profs. Carlo Sèquin, Sara Beckman, Alice Agogino, and Paul Wright for their time and efforts in shaping my proposal. I also appreciate Prof. Sequin and Prof. Agogino's time for serving on my dissertation committee.

I would not be writing this thesis if my parents did not share my dreams and aspirations. I am privileged to have their unwavering support. Along with my parents, my wife Purva Ghate has taken tremendous efforts in supporting and encouraging me throughout the last five years; I cannot thank her enough.

Finally, and most importantly, I thank my adviser for everything she did during my studies at UC Berkeley. She partially funded my work, advised me on courses, guided my research, mentored me when I was a GSI, and also taught me to communicate correctly and effectively in American English with unmatched patience. Thank you Professor Sara McMains.

Chapter 1

Introduction

It is estimated that industrial manufacturing causes 19% of global greenhouse gas (GHG) emissions [Herzog 2005] and 31% of U.S. energy use [U. S. Energy Information Admin. 2008]. As industrial manufacturing progressed from craft to mass and further to lean production, machine tools increasingly replaced human powered processes. Most manufacturing machine tools in industry today are powered by electricity [Mori et al. 2011].

Although virtually clean to consume (when compared to burning coal or oil), electricity is not a truly clean energy source. In the US, even today, the majority of electricity is generated by burning non-renewable fossil fuels. Similarly in China — the leader in industrial manufacturing — more than 60% of electricity is still generated from coal, causing a chronic and widespread layer of smog above Eastern China [World Nuclear Association 2013]. Thus, for long term energy independence and also to reduce GHG emissions that cause global warming [Herzog 2005], we must curb energy demand in manufacturing.

However, steps to reduce energy consumption in manufacturing cannot adversely affect the economics of business. In other words, when reducing energy consumption, productivity of industrial manufacturing processes must be maintained or improved. No industry can revert to craft production for saving energy while still being competitive in the modern world. Consumers too will never accept products of lower quality or delayed deliveries in lieu of a cleaner manufacturing process. Therefore, research must find answers to this dilemma: how to achieve economic growth while protecting the environment [Gutowski et al. 2001]?

1.1 Research Motivation

In the past century, productivity-driven academic and industrial research has transformed the manufacturing industry. For example, research on lean manufacturing, as reported in “The Machine that Changed the World,” has identified and removed many *muda* or waste-causing practices from traditional American automobile manufacturing [Womack et al. 2007], enabling American companies to regain competitiveness in the global market. As a result of a vast body of research on manufacturing processes, most manufacturing processes are now well-studied in terms of their productivity aspects. Ironically, though, only scant research

can be found in the literature focused on reducing energy consumption in manufacturing processes [Dufflou et al. 2011]. Thus, in this century, we must put forth the objective of energy efficiency as well as productivity when researching new and existing manufacturing processes. In this dissertation, we study CNC milling with this combined objective.

1.2 CNC Milling and Energy Consumption

Milling is one of the older, popularly used, traditional manufacturing processes that use a rotary cutter to shape a surface being fed into the cutter [Usher 1896]. It is implicitly assumed that milling is performed on a “machine” powered by electricity. Milling machines have evolved significantly since this 100 year old definition to today’s modern machines that can perform complex simultaneous 5+ axis operations and maneuvers requiring computerized numerical control (CNC).

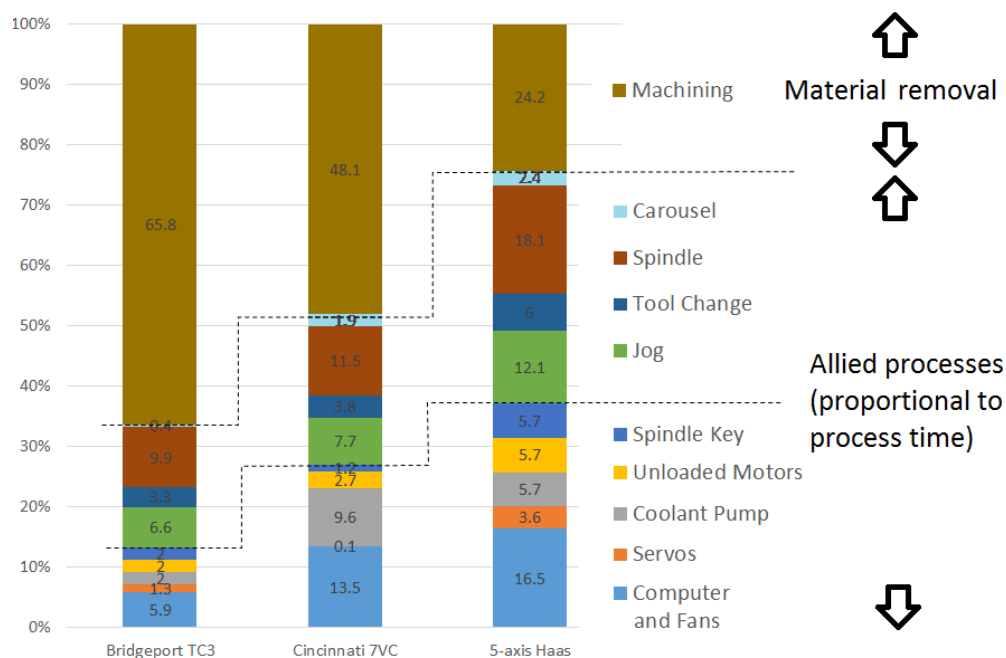


Figure 1.1: Energy consumption profiles of three different CNC machines. (Data from [Kordonowy 2002])

Although still electrically-powered and operating on the same basic principles, modern CNC milling machines are significantly different from older milling machines. [Kordonowy 2002] studied several generations of milling machines in order to compare their electrical performance. Their work confirms that not all CNC milling machines are equivalent when electricity consumption is considered. Figure 1.1 is plotted to compare three select results from Kordonowy’s thesis simultaneously. It can be seen that the oldest Bridgeport TCS, a 3-axis machine, spends most of the consumed energy (65.8%) on material removal processes,

while in the case of the newest Haas 5-axis machine, only 24.2% of the total drawn energy is spent on material removal. The Cincinnati machine falls in between the two, spending about a half of the drawn energy on material removal. Collectively, we draw two inferences from the figure:

1. Various sources of electricity consumption in CNC machines can be roughly classified into two categories: (a) sources that draw power highly dependent on material removal operations and (b) allied processes that draw constant power proportional to the operation time.
2. As machines become increasingly advanced (Bridgeport 3-axis \rightarrow Cincinnati \rightarrow Haas 5-axis), the fraction of energy spent (or available) for material removal decreases, while a larger fraction of energy is spent on non-machining, allied processes that draw a fixed amount of power irrespective of the cutting activity (e.g. lights, fans, computer).

These inferences suggest an interesting direction for research on energy consumption in CNC milling. In the case of smaller machines like the Bridgeport, research is required to analyze the material removal process for its energy consumption effects, while in the case of advanced machines such as the Haas, the most impact on reducing energy consumption may be obtained by further research focused on reducing operation time. This idea forms the basis of this dissertation.

1.3 Research Outline

This research is primarily aimed at analyzing, modeling, estimating, and reducing energy consumption in CNC milling. We address all point-milling type operations where the cutter has a single point of contact with the workpiece during cutting (as opposed to flank milling¹ where the cutter has a line contact with the workpiece). Our goal is to develop the required knowledge and algorithms to analyze the performance of multi-axis CNC point-milling processes with respect to both economic and environmental objectives. Since CNC machines differ significantly in construction and energy usage, we realize that no “silver bullet” methodology can work across the range. Therefore, we divide them into two types — smaller (3-axis) and advanced (5+ axis) CNC machines — in this dissertation.

Chapter 2, we develop the required background and theory for both 3- and 5-axis CNC milling. 3-axis CNC milling machines are popularly used due to their high productivity and accuracy. However, no commercial tools exist to estimate or simulate their electrical performance to determine operating conditions that optimize cost and environmental impacts. With this aim, in Chapter 3, we first propose an analytical model of CNC milling derived from the first principles for metal cutting as well as from experimental observations. We derive various relationships that are used in developing our model and also demonstrate the procedure to customize our model to a new CNC machine. Following the model theory,

¹See [Ahmadi and Ismail 2010] for details on flank milling

in Chapter 4, we describe an application of the model: a software tool that can estimate energy consumption for a proposed machining operation for any 3-axis CNC milling machine. In Chapter 5, we demonstrate the value this software adds to a shop-floor by demonstrating several case-studies. We show the effects of process planning decisions on energy consumption in CNC milling operations in each of the presented case-studies. Learning from the results of the cases, we propose the concept of generating “inherently energy-efficient” toolpaths and present a proof-of-concept test case that demonstrates significant energy saving.

As evident in Figure 1.1, 5-axis CNC milling machines are significantly different when we compare the fraction of energy used in material removal. Due to significant overloads such as the computer, fans, lights, controllers, and idle servos, machining time dominates the energy consumption behavior of 5-axis CNC milling machines. Therefore, saving time in machining has the most impact among all approaches to saving energy. With this objective, in chapter 7, we describe a configuration-space based unified problem formulation and solution methodology for 5-axis toolpath planning to optimize the machining time. In addition to machining time or toolpath length, our approach to 5-axis toolpath planning offers process planners the ability to generate toolpaths while optimizing a combination of objectives. We also demonstrate an implementation of the proposed formulation and solution strategy for a lower-dimensional variant of the full 5-axis toolpath planning problem that was specially designed to ease visualization of the process.

Chapter 2

Background and Related Work

2.1 Preliminaries

We define CNC milling as milling operations performed on machines whose axes, spindle, and other mechanisms are controlled by a computer (CNC controller) that may be programmed using NC code. NC code is an universally accepted plain-text set of standard commands that a CNC controller is able to interpret to actuate machining. An NC code is made up of G/M commands, positional coordinates, and other numerical values. For this dissertation, we only use generic G/M commands that are common to most CNC machine controllers such as FANUC, Mori-Seiki, Siemens, etc. CNC milling machines are classified according to the number of axes the cutting tool (cutter) can simultaneously move in. 3-axis CNC machines have three translational degrees of freedom (DOFs), while 4- and 5-axis CNC machines have one or two additional rotational DOFs, respectively. In this dissertation, we only address two groups of CNC machines: 3-axis or 5-axis. However, all discussion about 3-axis machines is readily applicable to 2- and 2.5- axis machines, while the treatment for 5-axis machines can be extended to 4-axis and 5+ axis machines. In the next section we describe working of CNC machines with special emphasis on their energy consumption behavior.

2.2 Energy consumption in CNC machines

Most CNC machines rely on electricity as the chief power source [Mori et al. 2011]. As depicted in Figure 1.1, the electric power drawn by a CNC milling machine from a grid is the summation of electricity drawn by its sub-systems. Figure 2.1(a) and (b) show simplified graphs of power drawn by typical 3- and 5-axis CNC machines at various times in a typical machining operation. Once a machine is turned on, its lights, computer fans, and the controller begin consuming electricity at their rated power until the machine is switched off (idle power state). Additional energy is required to warm up the machine (jog) by running a predefined set of commands during initialization. After warm up, NC codes

may be executed to perform machining. When an NC code is executed on a machine, the machine draws additional electric power from the grid, as needed, for rotating the spindle, moving the axes, exerting cutting forces, and running the coolant circuit. The machine returns to its ready state once the NC code execution is complete and remains in that state until turned off. The two slender “spikes” of power consumption, also shown in the graphs, are due to activation of inductors in electric motors. The area under the power-time curve is the total energy consumed.

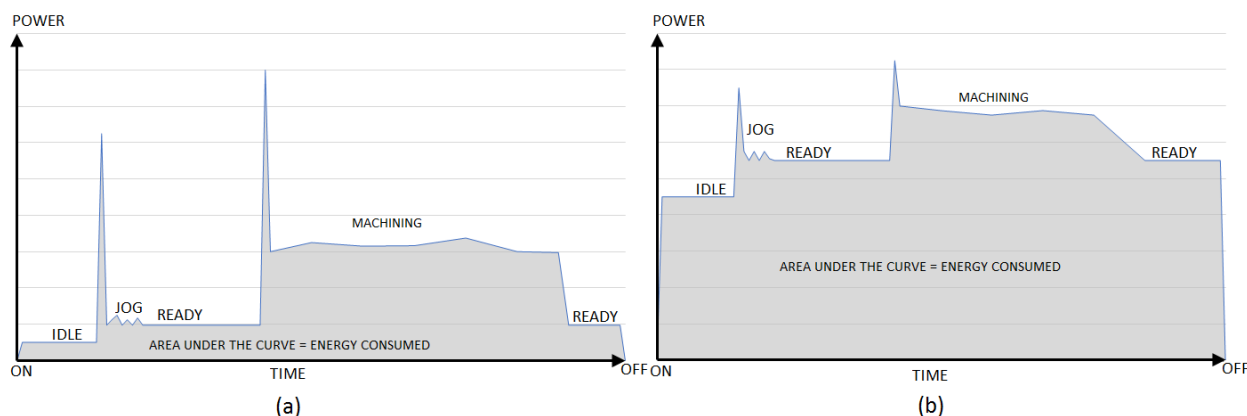


Figure 2.1: Power drawn by a CNC machine as a function of time (symbolic) (a) 3-axis machine, (b) 5-axis machine.

Although the power states mentioned above are common to every CNC machine irrespective of the number of axes, 5-axis CNC machines differ significantly from 3-axis machines when the share of each power state in the total power consumption is compared. Due to additional DOFs and larger size, many sub-systems in 5-axis machines (e.g. the axis servos) must be constantly energized (even if not moving) to maintain accuracy. Also, a sophisticated control system, dampening system, and position control sensors are necessary in 5-axis CNC machines for repeatable precision. Thus, the ratio of power consumed in machining to that spent as idle power is small in 5-axis machines. On the other hand, 3-axis machines are simpler in construction, control, and sensor systems, resulting in small idle power requirements. When 3-axis machines are used to cut metal, however, the amount of power required is larger, 5-7 times the idle power. Therefore, in 3-axis machines, most of the total energy consumed depends on material removal processes, while in the case of 5-axis machines, this seems to be of relatively less significance. Specific to the two machines in Figure 1.1, the Bridgeport and the Haas, a 50% reduction in energy spent in machining (material removal) results in about a third of total energy saved in the case of the 3-axis Bridgeport machine, while only about 12% saving in the case of the 5-axis Haas CNC machine.

In the next two sections, we outline the past work for each of the two types. First, in section 2.3, we describe work related to analyzing the 3-axis milling process, with an

emphasis on analytical energy models. Then, in section 2.4, we review toolpath planning methods for 5-axis machining to optimize machining time or total path length.

2.3 Analysis and modeling of the 3-axis milling process

We classify the analysis and modeling of the 3-axis milling process in the literature into four major types of process models: mechanistic force models, measurement-based models, hybrid models, and most recently, energy models for CNC milling.

Mechanistic models: [Martellotti 1941, Merchant 1944] developed theories based on cutting forces for point-contact machining processes such as milling, turning, grinding. These models can be used to predict stable and unstable machining conditions (e.g. stability lobes proposed by [Tobias 1965]).

Measurement-based models: [Altintas 1992] and [Tlusty and Ismail 1981] proposed milling process models based on comprehensive experiments with various objectives such as to minimize chatter (vibrations) or to maximize tool life. Some other measurement-based models, e.g. [Balogun et al. 2013], were based on experimental measurements on multiple CNC machines to determine the relative performance of the machines in similar processing conditions.

Hybrid models: [Feng and Menq 1994] reported a model for ball-end milling based on mechanistic principles and measured forces. [Tonissen 2009] proposed a model based on Merchant’s cutting theory that also used experimentally determined constants for customized predictions. [Yang and Park 1991] presented a model based on geometric analysis of a ball-end mill’s cutting edge to estimate cutting forces.

Most of the measurement-based and hybrid models rely on empirical constants to incorporate the effect of real-world conditions when making predictions. [Yun and Cho 2000, Azeem et al. 2004, Budak et al. 1996], among others, have provided methods to determine such empirical constants, called cutting force coefficients, from cutting experiments.

Energy models: [Gutowski et al. 2006] introduced a seminal energy model for CNC milling with the notion of modeling energy use in cutting based on the material removal rate (MRR). MRR has since been popularly used in estimating energy requirements by many researchers. [Kara and Li 2011, Diaz et al. 2011, Newman et al. 2012] have developed models using MRR to compute specific energy (i.e. energy required to remove a unit volume of material) in CNC milling, while [Mori et al. 2011, He et al. 2012, Balogun and Mativenga 2013] have developed MRR-based models to estimate energy requirements in machining an entire component.

Most analytical process models reported above consider the actual metal cutting process as an aggregate function of MRR but rarely isolate the contribution of individual process parameters, as partially done by [Newman et al. 2012]. Physical machine construction and toolpath geometry also affect energy consumed in machining as observed by [Altintas 1992, Balogun et al. 2013], but most energy models consider only simple toolpaths (e.g. [Balogun et al. 2013, He et al. 2012]), and do not test the effect of toolpath parameters, toolpath strategy, milling direction, or machine construction when modeling energy consumption. Our

work on modeling energy consumption in 3-axis CNC machines falls in the fourth category of models but our model also uses some relations derived in [Altintas 1992], a measurement-based model. Additionally, our model is different from the existing models because we aim to perform machine-specific, individual process parameter based, geometric analysis of NC toolpaths. We explain our 3-axis energy model in Chapter 3.

2.4 Toolpath planning for 5-axis machines

5-axis CNC machines are most suited for manufacturing freeform or sculptured surfaces and commonly used in the aerospace, automotive, energy generation etc. industries. 5-axis machines are different from 3-axis machines in their energy consumption behavior (as seen in Figure 2.1) since a larger fraction of the energy is consumed at a constant rate, irrespective of material removal requirements. Thus, reducing operation time (cycle time) is likely to have a larger impact on reducing overall energy consumption than merely reducing energy consumption in machining state (material removal). A vast body of research on programming 5-axis machines aimed at improving operation time can be found in the literature. A brief survey is compiled in the next section to introduce the state of the art in this area.

5-axis point milling is characterized by a single point of contact (CC) between the rotating cutter (located at cutter location CL) and the surface being machined. The cutter is programmed to follow a fixed sequence of CL points (toolpath) above the surface. Figure 2.2 illustrates these terms for flat and ball-nose end-milling cutters.

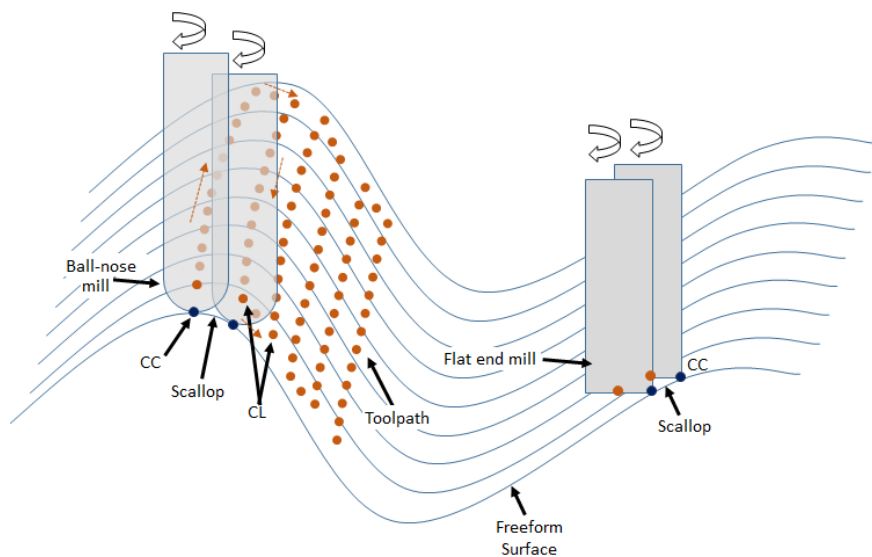


Figure 2.2: Cutter location (CL), cutter contact (CC), toolpath and scallop in point milling of a freeform surface

Toolpath planning for 5-axis machining consists of two sub-problems: toolpath generation

(location and connectivity of CL points) and tool orientation computation. Both sub-problems are widely studied in the literature; surveys of related research can be found in [Jensen and Anderson 1996, Dragomatz and Mann 1997, Lasemi et al. 2010]. In Table 2.1, we have compiled a list of relevant research works in either of the two sub-problems, classified according to the technique used.

Toolpath generation: The objective in the toolpath generation sub-problem is to determine a set of CL points, their connectivity, and toolpath parameters (e.g. path overlap) to ensure complete machining of the desired freeform surface in the least machining time.

Methods for computing CL points/path were initially derived from 3-axis toolpath planning methods that assumed a fixed orientation of the cutter. Basic methods such as axis-parallel zig-zag toolpaths, contour-parallel spiral toolpaths, and their variations such as space-filling curves were initially used for generating CL points from the design surface geometry. Later, iso-parametric, iso-planar, and iso-scallop toolpath planning strategies were developed by sampling points on the input surface in various ways. Methods were also developed for non-parametric inputs, compound surfaces, and special materials that heavily relied on the geometry of the input design surface. Most of the CL path computation strategies extended from 3-axis machining have limited applications in 5-axis machining because they require complete accessibility of the surface. Some comparatively newer methods do not assume complete accessibility of the workpiece surface and are thus suited for true 5-axis machining components such as turbine blades. These include curvature matched machining and other curvature-dependent methods, use of isophotes, and some other geometric techniques that improved productivity by optimizing material removal. Some techniques use geometric information to transform the toolpath planning problem into an optimization problem in the configuration space (C-space) of the cutter.

Dedicated methods to compute toolpath parameters (such as forward step, side step, and feedrate) are also found in the literature. These methods assume an underlying toolpath topology when computing toolpath parameters for increased productivity.

Tool orientation computation: Tool orientation computation techniques take CL points and toolpath parameters as their input (along with the design surface) to compute tool orientation angles such that no gouging occurs at any CL point. Several techniques based on computing the tool shadow region aimed at preventing local/rear gouging and reducing computations in the process. Curvature matching based methods were also proposed that ensured non-gouging toolpaths by matching the equivalent tool curvature with the local surface curvature. Additionally, some methods optimized material removal by minimizing deviation from the surface normal. For more complex components that required global gouging checks, configuration-space (C-space) based methods were proposed. A few other strategies explicitly modeled the tool orientation sub-problem as an optimization problem. Finally, some methods assumed an input of feasible orientations to iteratively determine a smoothed set of orientations such that orientation changes were minimal and gradual.

This treatment of the full 5-axis toolpath planning problem as a sequential problem of computing a CL path followed by tool orientations implicitly assumes that the two sub-problems are independent of each other. However, this is not the case, as concluded by

several researchers including [Wang and Tang 2007].

2.4.1 Interdependence of sub-problems

Although seemingly independent of each other, the two sub-problems of finding cutter locations and cutter orientations are actually inter-dependent. [Jun et al. 2003] have showed that the choice of cutter location points affects the feasible range of tool orientations. Conversely, several alternative cutter locations may be obtained to machine the same CC point by merely varying the tool orientation [Jensen 1993]. Therefore, solving the two sub-problems independently or sequentially can never lead to a truly optimal solution of the complete problem [Wang and Tang 2008, Barakchi Fard and Feng 2009].

Formulating and solving the full 5-axis problem that solves both sub-problems simultaneously is a daunting task. The full problem must solve for cutter locations, connectivity, and cutter orientations simultaneously, while optimizing machining time, material removal rate, and machining quality. However, just finding connectivity of CL points alone is an NP hard problem [Castelino et al. 2003]. Therefore, researchers devise and solve parts of the full problem while assuming a solution for the remaining. Most commonly, as seen in Table 2.1, either the toolpath planning sub-problem or the tool orientation planning sub-problem is solved independently.

2.5 Summary

In this chapter, we described the working of CNC machines, characteristics of their constituent sub-systems, and differences in their electricity consumption behavior that separate 3-axis machines from 5-axis machines. We identified that in 3-axis CNC machines, the majority of energy is spent in material removal processes (40-60%). Existing research on analytical process models, particularly for energy modeling in 3-axis machines, identifies multiple power states of a CNC machine when simulating or estimating energy consumption. Energy required for material removal is only calculated as an aggregate, proportional to the MRR in the process. Most of the proposed models perform reasonably well for standardized components/toolpaths but no model considers (or can be directly extended to consider) the effect of toolpath geometry and machining parameters on energy consumption in 3-axis machining.

In 5-axis CNC machines, most of the energy is spent on non-machining processes, resulting in higher idle power consumption, irrespective of machining operation. Therefore, in 5-axis machines, energy saving may be best realized by reducing the operation time. Toolpath planning for 5-axis machining with the aim of minimizing operation time consists of solving two sub-problems: toolpath planning and tool orientation planning. Several independent approaches exist for solving either sub-problem independently, but due to the problems' inter-dependence, a truly optimal solution can be obtained only if both sub-problems are simultaneously solved. Such a formulation and solution is still an unsolved problem.

Table 2.1: Past work on 5-axis machining of freeform surfaces

Toolpath generation	CL path planning	Extended from 3-axis	Basic: Zig-zag [Marshall and Griffiths 1994, Misra et al. 2005], Contour parallel [Held et al. 1994], Space-filling curves [Anotaipaiboon and Makhanov 2008], Adaptive space-filling curves [Makhanov 2009], Air-time minimization [Castelino et al. 2003]
			Geometric: Iso-parametric [Lo 1999], Iso-planar [Feng and Teng 2005], Iso-scallop [Suresh and Yang 1994], Adaptive iso-curves [Elber and Cohen 1994]
			Special purpose: Trochoidal [Elber et al. 2005a], Non-plunging [Rauch et al. 2009]
			Non-parametric input geometry: [Lu et al. 2008, Kiswanto et al. 2007, Balasubramaniam et al. 2000, Sun et al. 2001]
			Compound surfaces [Sarma and Dutta 1997, Veeramani and Gau 1998, Chen et al. 1993]
	5-axis machining specific	Curvature-based: Curvature matched machining [Jensen 1993], Curvature loci [Giri et al. 2005], Machining Potential [Chiou and Lee 2002]	
		Isophotes [Han and Yang 1999, Han et al. 2001]	
		C-space based [Choi et al. 1997, Morishige et al. 1997, Lu et al. 2008]	
	Process parameters	Pitch, side steps	Surface error based [Li et al. 2007], Pitch and orientations [Farouki and Li 2013]
			Artificial immune system [Ulker et al. 2009]
Tool orientation computation	Tool orientations	Shadow based	
		Rolling ball method [Gray et al. 2003]	
		Arc intersect method [Gray et al. 2005; 2007]	
	C-space	Machining strip width [Barakchi Fard and Feng 2009]	
		Isoconic [Wang and Tang 2007]	
	Optimization	Curvature based	
		Curvature matching [Jun et al. 2003, Pi et al. 1998]	
Orientation smoothing	Minimizing changes	Least squares [Chen et al. 2009], Relative normal curvature [Gong et al. 2010], Evolutionary multi-objective [Kersting and Zabel 2009], Kinematic error [Budak et al. 2009, Ye and Xiong 2008], Inverse kinematics [Farouki et al. 2013]	
		C-distance [Jun et al. 2003], quaternion interpolation [Ho et al. 2003], visibility maps [Wang and Tang 2008], tool marks [Chen et al. 2009] Pitch and orientations [Farouki and Li 2013]	

Chapter 3

Modeling Energy Consumption in 3-axis Milling

If you cannot measure it, you cannot improve it. - Lord Kelvin

In our quest to reduce energy use in machining, we first analyze the energy consumption in its present state to understand exactly where and how the energy is spent. In this chapter, we develop this knowledge in the form of an analytical process model of CNC milling. We first define the nomenclature that we will use in our derivations and applications in Chapters 3-5.

Nomenclature

N_s	: Spindle speed
F_i	: i axis feedrate
d	: Depth of cut
w	: Width of cut
D	: Cutter diameter
MRR	: Material Removal Rate
F_c	: Cutting force
P_j	: Instantaneous power consumed by sub-system j
E_j	: Energy consumed by sub-system j
T_i	: Time consumed by sub-system j

3.1 Past work on modeling CNC milling

We briefly outlined the past work on modeling the CNC milling process in section 2.2. In this section, we further explain models under the fourth type — energy models — since they are the most relevant to our work. A generalized representation of most existing models can

be made in the form of:

$$E = \sum_i PowerState_i \cdot time_i, \quad (3.1)$$

where E is the total energy required, and $PowerState_i$ and $time_i$ are various power states and corresponding time intervals. Following are specifics of some prominent analytical models.

- [Gutowski et al. 2006] define a single power state and time interval as

$$E = (P_0 + K \cdot MRR) \cdot t,$$

where P_0 represents the portion of total energy consumed at a constant rate, while $K \cdot MRR$ represents energy required for material removal proportional to the MRR . Use of MRR has since become the norm when modeling energy usage in machining.

- [Diaz et al. 2011] present a model based on separating cutting and air (non-cutting) power states to obtain an averaged power state for the entire time:

$$E = P_{avg} \cdot t = (P_{cut} + P_{air}) \cdot t.$$

- [Mori et al. 2011] identify three power states: basic, cutting, and air-cutting (positioning) power, where they too compute the power requirement of the cutting state using MRR . The total process time is divided into cutting and air-cutting times, each used separately for the respective cutting states. Thus their model can be expressed as:

$$E = P_{basic} \cdot (t_{cutting} + t_{air}) + P_{cutting} \cdot t_{cutting} + P_{air} \cdot t_{air}.$$

- [Balogun and Mativenga 2013] separate the machine's power state into three (partially) overlapping power states of basic, ready, air-cutting, and machining/cutting. This model, too, uses MRR and a proportionality constant k to compute energy used in material removal.

$$E = P_{basic} \cdot t_{basic} + (P_{basic} + P_{ready}) \cdot t_{ready} + P_{air} \cdot t_{air} + (P_{basic} + P_{air} + P_{cool} + k \cdot MRR) \cdot t_{cut}$$

- [He et al. 2012] present a model that explicitly computes energy for various sub-systems of the machine by considering the total time each sub-system is active. They also introduce explicit computation of the power drawn by the spindle sub-system (P_{sp}), the power drawn by the tool-change mechanism (P_{tc}), and the tare power ($P_{servo} + P_{fan}$).

$$E = \int_{t_{sp}} P_{sp} dt + \int_{t_{cut}} P_{cut} dt + \sum_{i=1}^m \int_{t_f} P_i dt + P_{cool} t_{cool} + P_{tc} t_{tc} + (P_{servo} + P_{fan}) t$$

We identify the following key characteristics of this past work:

1. Most previous models compute the power required for material removal from the MRR during machining, with or without empirical constants. We intend to explore if there may be additional research opportunities to study the effect of individual process parameters as well as the geometric aspects of the toolpath in the milling process. The process parameters include feed, depth of cut, width of cut, and up/down milling direction (for details, see [Trent and Wright 2000], Chapter 2) while the geometric aspects include number of corners, path lengths, prominent cutting direction, and toolpath strategy.
2. With the exception of [He et al. 2012], no model proposes computing the required power for feeding or rapid travel separately in the X, Y, and Z directions. This results from an implicit assumption that the energy required to remove material or move the axes is the same in all three principle directions of motion (X, Y, and Z). In practice, however, this assumption does not hold. Generally, the two axes of the table, for example, have different masses, different bearings, different motors, and different mounting configurations (one of the axes is typically mounted on top of the other) that make movements of the axes require different amounts of force (thus different electric power) depending on the direction of motion.
3. Most previous models are based on constants or conditions that restrict their applicability to the particular machine used in the research. The experimental procedure to compute the constants required to apply these models to a new machine or manufacturing conditions are rarely described. Thus, most models cannot be readily used on a large variety of CNC machines, outside the research group.
4. Some models use power readings and other parameters from machine handbooks (e.g. [He et al. 2012]) that may not be easy to obtain or may not be up to date (due to aging, maintenance, etc.) in an industrial setting, further restricting commercial use of these models in industrial CAD/CAM software. Based on our experience when working with industrial research collaborators from Audi AG, we found that it is often too difficult or impossible for industrial partners to invest resources and time to find the exact machine parameters. Thus, for easier adaption in the real-life scenarios, we must develop a model that stands on its own, without the need of any machine handbook data.

In developing a new energy model for CNC milling, we address some of the above concerns by moving away from empirical constants and parameters obtained from machine handbooks to develop a model that explicitly computes energy consumption in each activity during machining of a workpiece. We also introduce a “customization” method to extend the application of our model to any CNC machine with a one-time customization step. We explain the details of our model in the following sections.

3.2 Our Proposed Model

Energy consumed by a CNC machine ($E_{machine}$) can be divided into:

1. E_{const} : components that consume energy at a constant rate, irrespective of the cutting operation (e.g. lights, computer, fans), and
2. $E_{variable}$: components that consume energy at a variable rate, depending on the cutting operation (e.g. energy for material removal, table movements, spindle rotation).

Thus, we write:

$$E_{machine} = E_{const} + E_{variable}. \quad (3.2)$$

Since the energy required in a machining operation can vary based on machining activities in the operation, we compute the total energy required by computing the energy requirement of each activity in its NC code (the program that a CNC machine sequentially executes in a machining operation). This is a new approach, also found in [He et al. 2012] but not implemented in any commercial CAD/CAM software. Most commercial CAD/CAM software instead generalize the manufacturing energy requirements only based on the part design (e.g. Solidworks [Dassault Systems 2013]). Since a part may be manufactured by multiple alternative methods, each possible requiring different machining time and energy depending on the operations performed, we believe that energy requirements to machine a part are better computed using the NC code used in its machining. Computing block-by-block energy usage from the NC code also allows us to incorporate the geometric aspects of the toolpath into the energy computation. The total energy demand is aggregated as a summation of those over all blocks in the NC code being analyzed:

$$E_{machine} = \Sigma E_{block}.$$

For each block of NC code, we write the energy consumption equation as:

$$E_{block} = P_{block} \cdot t_{block}, \quad (3.3)$$

where P_{block} is the electric power drawn by the machine from the grid and t_{block} is the machining time for that block (activity) in the toolpath. We compute t_{block} as done by [He et al. 2012], using an acceleration value of $a = 1m/s^2$. Most CNC machines used in the industry and academia have this limiting value for axis acceleration, both in our observation and as reported in the literature. Thus, as shown in Fig. 3.1, we consider a trapezoidal profile for feedrate, to make realistic time computation for each block, computing t_{block} as the addition of the time required for the axis to accelerate to the rated feed, move at the rated feed for the programmed distance, and decelerate (if needed) to the rated feed of the next block.

Similar to eq. 3.2, we further divide P_{block} as

$$P_{block} = P_{constant} + P_{variable}, \quad (3.4)$$

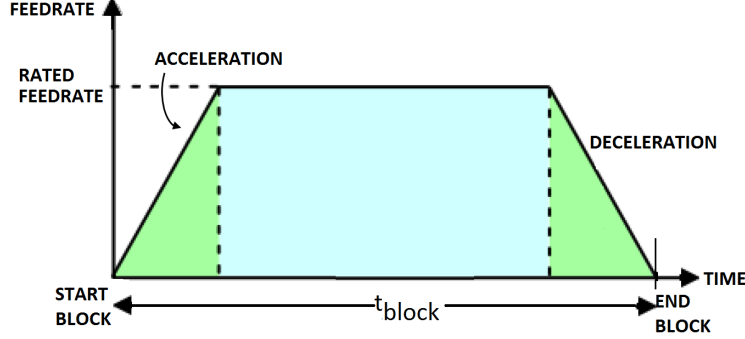


Figure 3.1: Computation of t_{block}

where

- P_{const} constitutes all components in the machine that draw power at a constant rate, irrespective of the cutting operation or toolpath. Examples of such components include the controller, lights, coolant pump, etc. For a block of NC code, depending on the state of the machine, one or many of these contribute a fixed amount of power to the total power consumption by the machine. In general,

$$P_{constant} = P_{tare} + P_{coolant_pump}. \quad (3.5)$$

- $P_{variable}$ constitutes the power drawn by the machine at a variable rate, according to the activity in the block. $P_{variable}$ is comprised of two major components: P_{moving_axes} , the power drawn by the machine to merely move (table movement, spindle axis movement, and spindle rotation), and $P_{cutting_force}$, the additional power drawn from the grid to exert the cutting force for removing material (if cutting happens). So,

$$P_{variable} = P_{moving_axes} + P_{cutting_force}. \quad (3.6)$$

Hence, combining the above equations,

$$P_{block} = P_{tare} + P_{coolant_pump} + P_{moving_axes} + P_{cutting_force}. \quad (3.7)$$

From our observations, the energy required for mere axis movements is directly proportional to the programmed feedrate F . Similarly, the energy required to rotate the spindle is proportional to the programmed spindle speed N_s according to our experiments and as reported in [Balogun and Mativenga \[2013\]](#).

Thus,

$$P_{moving_axes} = P_{spindle_rotation} + \sum_{i=x,y,z} P_{i_move}, \text{ where,} \quad (3.8)$$

$$P_{spindle_rotation} \propto N_s, P_{i_move} \propto F_i.$$

$P_{cutting_force}$, the additional power drawn from the grid to exert the required cutting force F_c , can be computed as follows. From first principles, not all the drawn power (energy) is converted into cutting force; some energy is always lost in overcoming Coulomb friction, in damping, and in waste heat. This treatment is identical to Equation 1 in [Altintas \[1992\]](#), where the authors state that an axis motor’s useful torque is spent in overcoming inertia, damping, friction, and the rest is converted to cutting torque. We have eliminated the inertia component because we considered it separately above in P_{moving_axes} . Thus, excluding the unmeasurable waste heat, we write:

$$P_{cutting_force} = P_{Coulomb_friction} + P_{damping} + P_{material_removal}. \quad (3.9)$$

We note from [Smith and Thusty \[1991\]](#) that the cutting force required to cut the material is directly proportional to the material removal rate MRR of the cutting process. MRR is a function of width of cut w , depth of cut d , and feedrate F . From [Altintas \[1992\]](#), Coulomb friction and damping are directly proportional to the exerted cutting force F_c . Thus,

$$\begin{aligned} P_{Coulomb_friction} &\propto F_c, \\ P_{damping} &\propto F_c, \\ P_{material_removal} &\propto F_c, \text{ and} \\ F_c &\propto MRR. \end{aligned} \quad (3.10)$$

Thus,

$$P_{cutting_force} \propto MRR. \quad (3.11)$$

These inferences of linear proportionality (in Equations 3.8, 3.10) were also verified experimentally in [Altintas \[1992\]](#), [Smith and Thusty \[1991\]](#), [He et al. \[2012\]](#), [Balogun et al. \[2013\]](#).

All discussion up to this point is independent of the construction, the size, and the scale of the CNC machine in question. In order to use the same basic analytical model for a wide range of CNC machines (e.g. from small retro-fitted CNC machines to huge industrial gantry-type machines), we provide a mechanism that incorporates machine-specific information into our model. This mechanism uses several experimentally-determined machine-specific constants to relate our analytical model to the CNC machine under analysis. These constants, called customization constants, are introduced for all proportional relations derived above in Equations 3.8 and 3.10. By introducing customization constants, we obtain linear equalities between the process parameters and their corresponding power usage contributions. For each such relationship, e. g. between any two variables ζ and ψ that are linearly proportional to each other, we introduce two constants KA and KB such that $\zeta = KA + KB \cdot \psi$. This form of linearity is similar to that used in models by [Layek et al. 2012](#) and [Diaz et al. 2011](#). Also, we compute the customization constants and the quantities P_{move} and P_{cut} as a summation of those for each of the three principal axes (X, Y, and Z). Such an individualized calculation for each axis helps in accurate consideration of toolpath geometry, since each axis may have a different mass and hence a different value

for customization constants.

Using the customization constants, our final model equation for P_{block} can be written as:

$$\begin{aligned}
 P_{block} = P_{tare} + P_{coolant_pump} + \sum_{i=x,y,z} (KA_{move_i} + (KB_{move_i} \cdot F_i)) \\
 + (KA_{spindle} + (KB_{spindle} \cdot N_s)) \quad (3.12) \\
 + \sum_{i=x,y,z} (KA_{cut_i} + (KB_{cut_i} \cdot MRR)).
 \end{aligned}$$

Use of customization constants enables us to use the same underlying model in Equation 3.12 for any CNC machine, once customization constants are determined for that machine. Further, since the constants are determined experimentally, the model does not rely on any manufacturer specifications or machine-tool handbooks. Also, a machine can be customized periodically to ensure that the model predicts energy estimates for the current state of the machine. The procedure to experimentally determine the customization constants for a CNC machine is described in the next section.

3.2.1 Determination of customization constants

Our main objective in defining customization constants is to individualize the analytical model to capture the electrical behavior of the machine under analysis as closely as possible. In essence, the customization constants represent the connection between our analytical model and the construction/working of physical sub-systems in the CNC machine in question. The constants are determined by performing a series of “unit operations” on the CNC machine and measuring the energy consumption with an in-line energy meter. [Behrendt et al. 2012] proposed a systematic approach to measuring and analyzing energy consumption in CNC milling. Many of our requirements are in line with their objectives. Therefore, we used the test component and measurement methods they recommend. We also ensure that constants are computed from samples over the entire working range of interest for the power state being analyzed. The procedure and the computations to determine the customization constants for the Haas VF-0 3-axis CNC milling machine in the Berkeley ME student machine shop is described below as an example of the process.

Objectives

For each new CNC machine, the model proposed above requires the following constants:

- $KA_{spindle}, KB_{spindle}$
- $KA_{move_x}, KB_{move_x}, KA_{move_y}, KB_{move_y}, KA_{move_z}, KB_{move_z}$
- $KA_{cut_x}, KB_{cut_x}, KA_{cut_y}, KB_{cut_y}, KA_{cut_z}, KB_{cut_z}$

- P_{tare} , P_{tool_change} , t_{tool_change}

In this section, we will find $KA_{spindle}$ and $KB_{spindle}$ values for the Haas VF-0 CNC machine. In Appendix A, we describe the complete procedure to determine the values of all customization constants for a new CNC machine to customize the analyzer for the new machine.

Apparatus

To measure electrical behavior, we need an energy meter with sufficient resolution and recording frequency. Ideally, we wish to capture the effect of every action/process/event that happens during the machine operation in an isolated setting. Also, since the measurements are for executing an NC code, the recording equipment must be able to correlate electrical events with events (blocks) in the NC code. Such electrical measurements are best performed by the same controller that parses and executes the NC code. This, however, is difficult to achieve with snap-on type laboratory-grade equipment that is not integrated into the CNC machine controller. Also, it is almost impossible to perform experiments on a perfectly isolated CNC machine tool (in the electrical sense).

[Behrendt et al. 2012] recommend using the Yokogawa CW240 energy meter for recording electrical measurements of NC codes as a reasonable alternative to controller-integrated energy measurements. The CW240 is capable of measuring and recording voltage, current, power factor, and power (numerically integrated) values for 3 phases and 3 wire loads simultaneously at 10 Hz. Since the CW240 cannot be synchronized with the NC code parser, we separate our experiments to record observations for a single parameter in each trial.

Experimental procedure and data processing

The energy meter (Yokogawa CW 240) measures all electrical parameters (e.g. phase currents, voltages, active power, etc.) during the trials and records the data. The most important electrical parameter for the purpose of our trials is the “active power” since that value represents the actual energy available to do work. The other values of reactive power and the rest of the power triangle are also available from a Yokogawa CW 240 but we do not use them in our research. Thus, henceforth in the dissertation we refer to the active power as the power drawn.

Figure 3.2 shows a typical plot of drawn power against time in an NC machining operation involving six linear cuts after starting from rest. We observe that there is a single large, slender spike/peak when the spindle is started, attributed to the energizing of the spindle motor coil. Following this, the six linear cuts can be identified by portions of steady power consumption with small power drops in between them when the machine momentarily stops (changes cutting direction). Additionally, there are six smaller peaks at the beginning of each linear segment (not noticeable in the Figure 3.2). In a similar but magnified plot, shown in

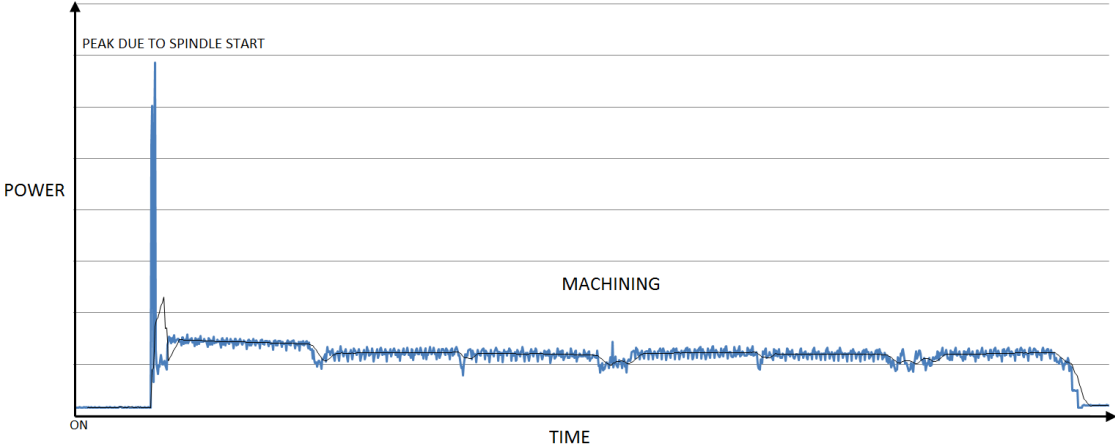


Figure 3.2: Typical power against time curve for a machining operation with six linear cuts indicating the starting peak/spike in power consumption when the spindle is started.

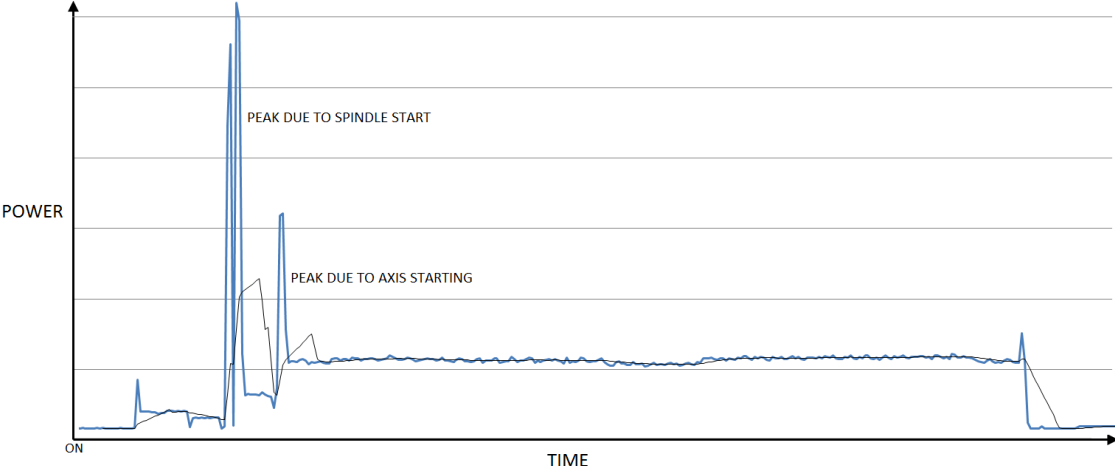


Figure 3.3: Typical power against time curve for a machining operation with a single linear demonstrating both, spindle and axis motor spike.

Figure 3.3, a separate smaller peak corresponding to starting of an axis motor is clearly seen for another machining operation involving a single linear cut.

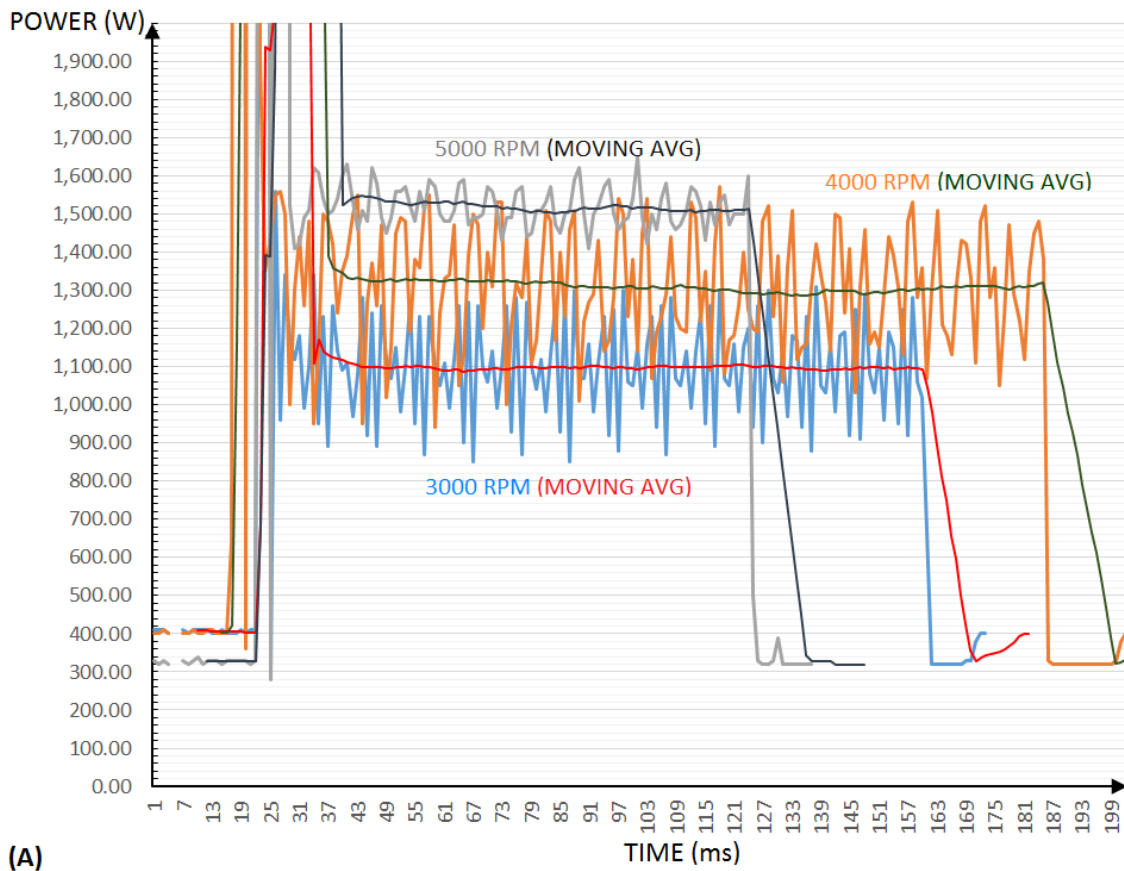
In this version of the energy analyzer, we ignore the spindle related peaks when computing energy consumption of an NC code because that event (spindle starting from rest) happens only a few times in an NC code. In contrast, the smaller peaks are noticed every time an axis motor is started so we consider and model those in our estimates by computing the time required for acceleration when computing t_{block} . For these customization trials, however, we mainly observe power values away from either types of peaks, when the machine has reached a relatively steady power state. Also, for each customization trial observation, we record three independent readings, approximated to the nearest tenth W.

We perform three measurements in this trial when computing $KA_{spindle}$ and $KB_{spindle}$ values for the Haas VF-0 CNC machine. The range of spindle speeds of interest for cutting aluminum by uncoated High Speed Steel (HSS) tools is 3500 RPM to 7500 RPM. To measure the customization constants, after connecting the energy meter in line, we operate the spindle (with a tool but without any load) at three different speeds in the range of operation. In each trial, the spindle is turned on for 6-10 sec. (the approximate time to achieve a steady value of power drawn after the peaks have subsided) and then turned off.

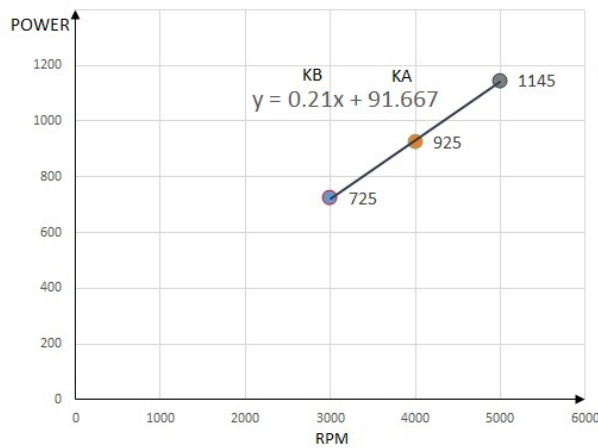
We then process data obtained from the Yokogawa CW240 to identify trends and various power states. We plot the (active) power values against time. To identify power states in the noisy power data, we compute the moving average (to counter the fluctuations in measurements) over the span of interest with a trend line. The moving average period for each trial depends on the spindle speed since each spindle rotation is a distinct electrical event marked by a “peak” in electricity consumption [Altintas 1992]. To ensure that the moving average is computed such that no partial current cycles are considered, we use a moving average period that is the smallest common multiple of spindle speed in RPS and 10, the measuring frequency of the meter. Thus, for the spindle speed of 4000 RPM, we use the moving average period of 12 (15 for 5000 RPM and so on).

Figure 3.4 (A) shows a combined plot of three trials, where active power values for each case are plotted against time. The three solid lines indicate moving averages for each of the three trials. From these plots, we observe that the machine drew 1100 W, 1300 W, and 1520 W (rounded to the nearest 10) when the spindle was rotating at 3000, 4000, and 5000 RPM respectively.

Now, the power drawn in these cases (1100 W, 1300 W, and 1520 W) is comprised of the constant power, P_{const} , and power required to rotate the spindle, $P_{spindle_rotation}$ (from Eq. 3.7). Thus, in order to determine $KA_{spindle}$ and $KB_{spindle}$, we first subtract the starting power state from each observation. For the Haas VF-0, the value of the starting power state was measured as 375 W. Thus, we compute $KA_{spindle}$ and $KB_{spindle}$ by fitting a straight line to the plot obtained by plotting $P_{spindle_rotation}$ values against corresponding spindle speeds (Figure 3.4 (B)). This plot, along with the obtained values of $KA_{spindle}$ and $KB_{spindle}$, is shown in Figure 3.4 (B). Similar experiments were conducted to determine other customization constants for the Haas VF-0 milling machine in the Berkeley ME student machine shop. In Appendix A, we describe the complete procedure to determine customization constants for



(A)



(B)

Figure 3.4: (A) Three superimposed plot of power values against time, recorded by a Yokogawa CW240 on a Haas VF-0 CNC milling machine. (B) Fitting a line to the moving averages of the power values.

a new CNC machine that uses a universal, parameterized component to cover all relevant motions as recommended by [\[Behrendt et al. 2012\]](#).

In the next chapter, we describe the development of software to analyze NC toolpaths for their expected energy consumption based on the energy model proposed in this chapter.

Chapter 4

Energy Model Applications

“Tools, metrics, and models to help sort out complex issues related to environmental concerns in manufacturing, to point directions, and to measure progress are badly needed.” - [Gutowski et al. 2005]

4.1 Background

In their study on large manufacturing corporations based in the US, Europe, and Japan, [Gutowski et al. 2005] found that corporations across the world were willing to transform manufacturing practices to address environmental concerns. However, even today’s CAD and CAM tools lack the ability to facilitate such transformations because they still maintain the conventional, purely productivity based view of manufacturing [Mittal and Sangwan 2013]. For example, mainstream CAD tools (e.g. Solidworks) to design/analyze components for structural, thermal, and mechanical performance lack the ability to correlate the effects of various design decisions to corresponding environmental impacts. Similarly in manufacturing, CAM software tools (e.g. ESPRIT) used in manufacturing process planning for maximizing productivity cannot provide any feedback for optimizing manufacturing processes to reduce environmental impacts. Although academic research on optimizing design/manufacturing activities with environmental objectives is abundant, rarely is the research implemented in a commercial CAD/CAM tool to make tangible progress toward environmental goals in industry [Bovea and Pérez-Belis 2012]. We address this need in this work, by developing an independent CAM software tool based on our energy model, that can be readily used in process planning to save energy in 3-axis CNC machining. In this chapter we explain various aspects of this software tool that uses the energy model we described in the previous chapter.

4.2 Energy analyzer software

In the previous chapter, we reported an analytical energy consumption model for 3-axis CNC milling that predicts the power drawn by a CNC machine at any stage of operation. Here, we use this model to develop a software tool that analyzes a planned machining operation to estimate the energy requirement of the entire operation. With these estimates, we aim to provide a means to correlate parameter and toolpath choices made in process planning of an operation to their effects on the energy (electricity) required for the operation. The intended users of this software are process planners, who can use this software along with toolpath planning software to make process planning decisions by simultaneously considering environmental and productivity objectives. We first describe the various software design decisions made when developing this software.

(Some of the ideas presented in this section were first introduced in our earlier version of the energy analyzer software with a different energy model in [Choi et al. 2009]. Yusuke Yasui implemented the analyzer first; we build on the same implementation in this dissertation but incorporate and implement our energy model for the analysis.)

4.2.1 Software Design

We made the following decisions when developing the energy analyzer software such that it can be readily used during process planning on a shop floor.

1. Individualized analysis: we designed the energy analyzer with an objective of making machine-specific energy requirement predictions, while still supporting a wide variety of CNC machines and machining conditions with the same underlying model. Therefore, in addition to the use of machine specific customization constants in the energy model, the software is designed to accept and incorporate case-specific inputs on toolpath generation parameters used in CAM software (e.g. typical percentage overlap), tool diameter for each tool, preferred milling direction when generating the toolpath, etc.
2. NC code (G/M commands) as input: This software is intended to be used after a process planner has generated an NC code for a component using any CAM software. Instead of computing “typical” energy required for manufacturing a part, merely based on the part geometry as done in many CAD/CAM software of the present day (e.g. [Dassault Systems 2013]), we analyze the generated NC code to make specific predictions of electricity requirements in manufacturing for the selected process conditions. This method provides case-specific feedback about the environmental impact of the part’s manufacturing, since the same part could be manufactured by a number of alternative methods/toolpaths, each possibly requiring different time and energy.
3. Block-by-block: We parse the provided NC code block-by-block to determine the time and energy requirements for each block separately using the energy model.

The cumulative sum of all blocks in the CNC code gives the total time and energy requirement of the CNC code. This method also allows us to visualize detailed analysis of the code for identifying the operations and their environmental impacts individually.

4. Support for common G/M commands: We support all commonly-used G/M commands in NC codes but do not support any controller-specific commands in the software. This approach allows the analyzer to be used on NC codes post-processed for any controller (e.g. Fanuc, Siemens, MoriSeiki, etc.).
5. Web-based implementation: We have implemented the analyzer as a web-based service to allow its use in a web browser. Thus, it can be readily accessed and used on a shop-floor, in geographically distributed manufacturing sites, places with limited computational power, etc. All data processing happens on a remote server and only the result plots are rendered on the client machine using Google Charts API.

The working of the energy analyzer software is illustrated with the help of a flow-chart (Figure 4.3) in the next sub-section.

4.3 Energy analyzer process flow

The energy analyzer estimates the time and the energy required to run the provided NC code on the specified CNC machine. To make machine-specific estimates, the energy analyzer uses machine-customization data and other user-specified parameters used in CAM software when generating the input NC code. In addition to estimates of energy (in KW-H) and time (in seconds), a graph showing block-by-block energy and time requirements is also provided as an output.

Figure 4.1 shows the process flow chart for the energy analyzer. The software accepts an ASCII text file NC code as its input. The provided NC code is first parsed to detect all the tools used in the complete operation using tool change command instances. Then, for each detected tool, the user is asked to specify a tool diameter and approximate overlap percentage that is later used in energy computations. The user may also specify other parameters that were used when generating the NC code in CAM software.

On providing the tool diameters and CAM software parameters, the main execution loop of the analyzer begins parsing the NC code for the second time, processing one block at a time, until the end of file is reached or a terminate statement code (M30) is read. During execution, the three power states of P_{const} , P_{move} , and P_{cut} in the proposed energy model (Equation 3.12) are continually updated by the software. For each block, E_{block} is estimated from P_{block} and t_{block} using Equation 3.3. The total energy and time estimates are updated after each block by adding the E_{block} and t_{block} values to E and T . In the next section, we illustrate the working of the energy analyzer using screen-captures for a test NC code.

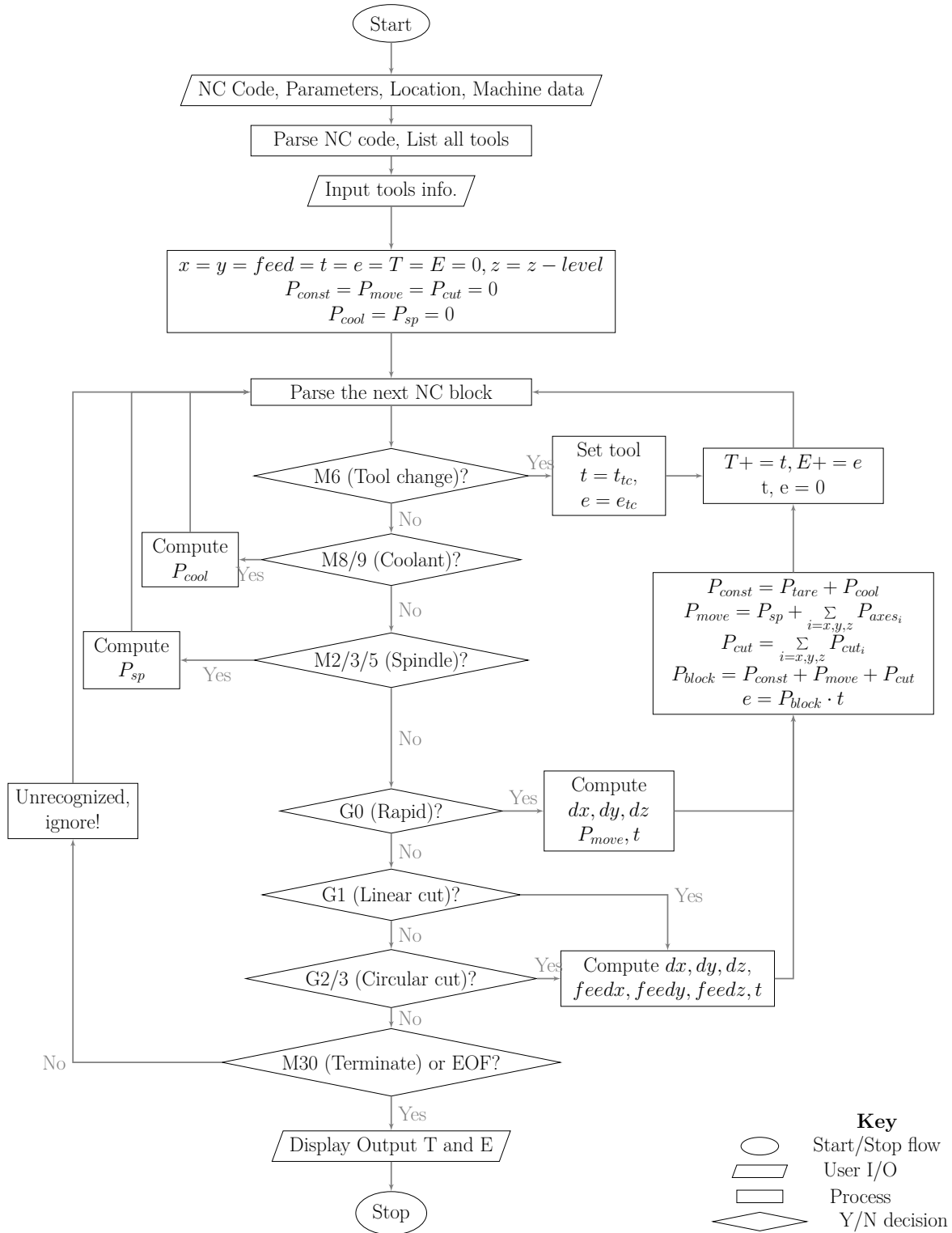


Figure 4.1: Flow-chart for the energy analyzer software

4.3.1 Software implementation and interface

We have implemented the energy analyzer in a client-server architecture so that it can be accessed in a browser using any capable device. The server-side scripting is done in PHP. The software internally uses Google Charts API [Google Inc. 2010-2014] to plot time and energy estimate graphs in a browser during output display. Following is a description of a typical run of a software to illustrate various steps in an analysis of an example NC code for milling a face of a rectangular block.

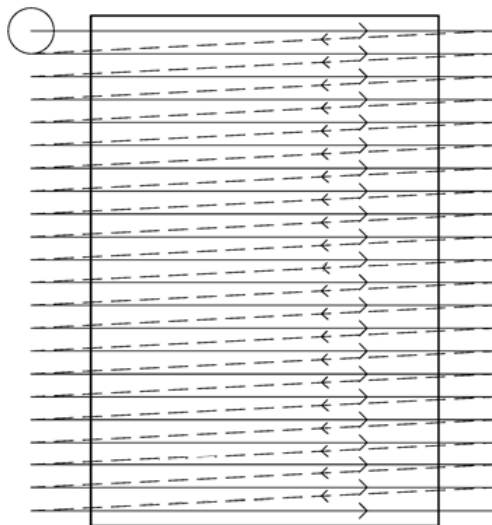


Figure 4.2: Face-milling a rectangular face

An analysis task begins with a user generated G/M code. For this example run, we analyze an NC code for a toolpath to mill a rectangular face by a single directional toolpath, parallel to X-axis direction (Fig. 4.2). We generated the toolpath in MasterCAM and verified its correctness, as seen in a screen-capture (Fig. 4.3). The complete NC code obtained from MasterCAM is attached as Appendix B.

Analysis

Analysis of a typical NC code, such as the one generated for facing in this example, starts with uploading the NC code to the energy analyzer web-portal. Figure 4.4 shows the input screen that appears after an NC code is uploaded. On this page, tool details, the starting z -level, and the typical programmed overlap in the uploaded NC code are obtained from the user. The user must provide tool diameters for each tool used in the NC code. Providing the remaining parameters (percentage overlap and z -level), however, is optional. If not provided (for example, if the NC code was hand-written), the energy analyzer uses the default values of 50% overlap and the z -level of 0.0.

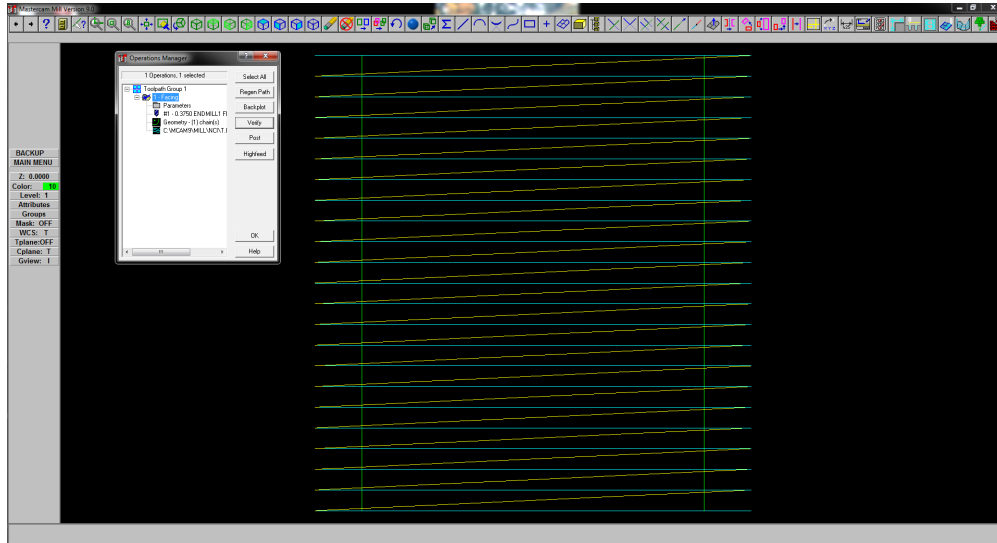


Figure 4.3: Generating and verifying toolpath for a facing operation in MasterCAM

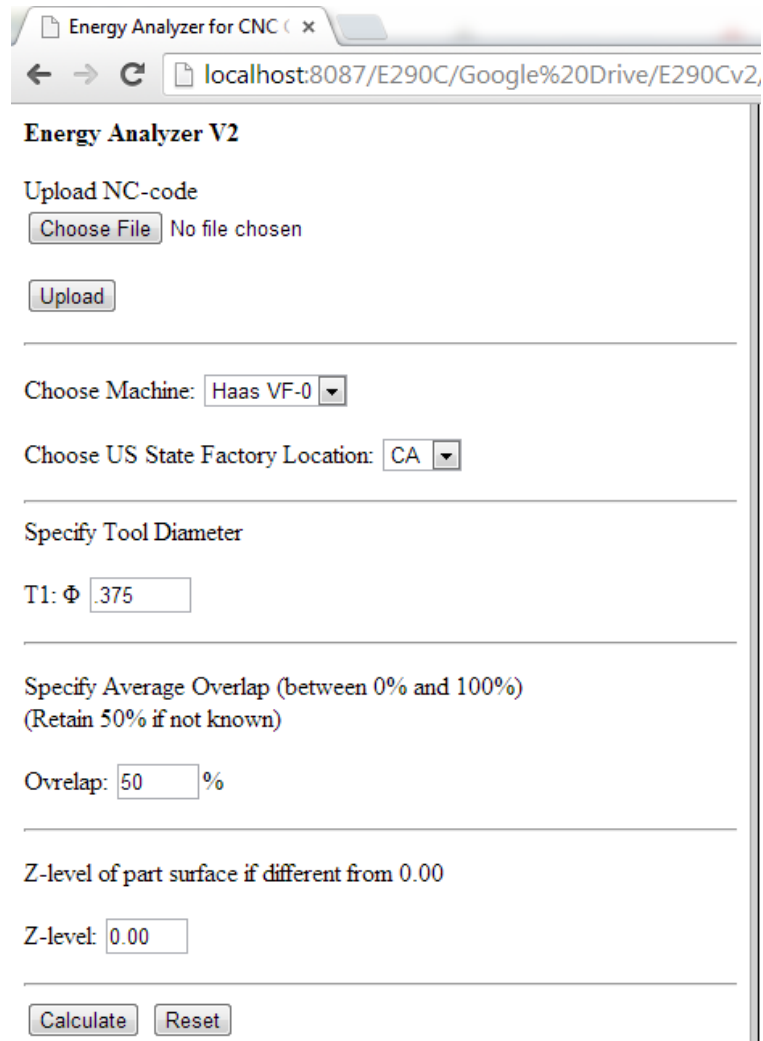
With these inputs and the NC code, the energy analyzer then computes the expected machining time (in seconds), required energy (in W-sec), and green-house gas (GHG) emissions (in Kg) based on United States Environmental Protection Agency (USEPA) data that relates the energy consumption to GHG emissions for 50 United States [U. S. Energy Information Admin. 2008]. The output screen includes two plots indicating expected block-by-block time and energy consumption. The output page for “FACE.NC” is shown in Fig. 4.5.

4.4 Validation of energy analyzer predictions

We performed additional validation experiments to corroborate the energy analyzer predictions with actual energy usage. The objective of these experiments was both to compare the total energy use as predicted by our software against the observed value, as well as to compare values of various power states predicted by the software against those observed instantaneously on an energy meter during actual machining.

The data presented here reflects values averaged over three (or more) trials for each experiment, since we want to avoid effects of fluctuations in the electricity supply. These validation trials were performed for a Haas VF-0 3-axis CNC machine in Berkeley ME student machine shop. In all trials, we used Aluminum 6061 workpieces and 2-fluted uncoated HSS end-mill tools of 0.375 inch diameter. As described earlier, we used a Yokogawa CW240 energy meter to record electricity consumption data such as the voltage, current, and power factor for each phase of the 3-phase electricity supply.

Also, to differentiate validation experiments from customization experiments, we measured various power states of the machine at different values of input parameters than those



The screenshot shows a web browser window titled "Energy Analyzer for CNC" with the address bar displaying "localhost:8087/E290C/Google%20Drive/E290Cv2". The main content area is titled "Energy Analyzer V2" and contains the following elements:

- Upload NC-code**: A "Choose File" button followed by the text "No file chosen", and an "Upload" button below it.
- Choose Machine**: A dropdown menu currently showing "Haas VF-0".
- Choose US State Factory Location**: A dropdown menu currently showing "CA".
- Specify Tool Diameter**: A text input field labeled "T1: Φ " containing the value ".375".
- Specify Average Overlap (between 0% and 100%) (Retain 50% if not known)**: A text input field labeled "Ovrelap:" containing the value "50" followed by a "%" symbol.
- Z-level of part surface if different from 0.00**: A text input field labeled "Z-level:" containing the value "0.00".
- At the bottom, there are two buttons: "Calculate" and "Reset".

Figure 4.4: User interface for providing toolpath parameters after uploading an NC code

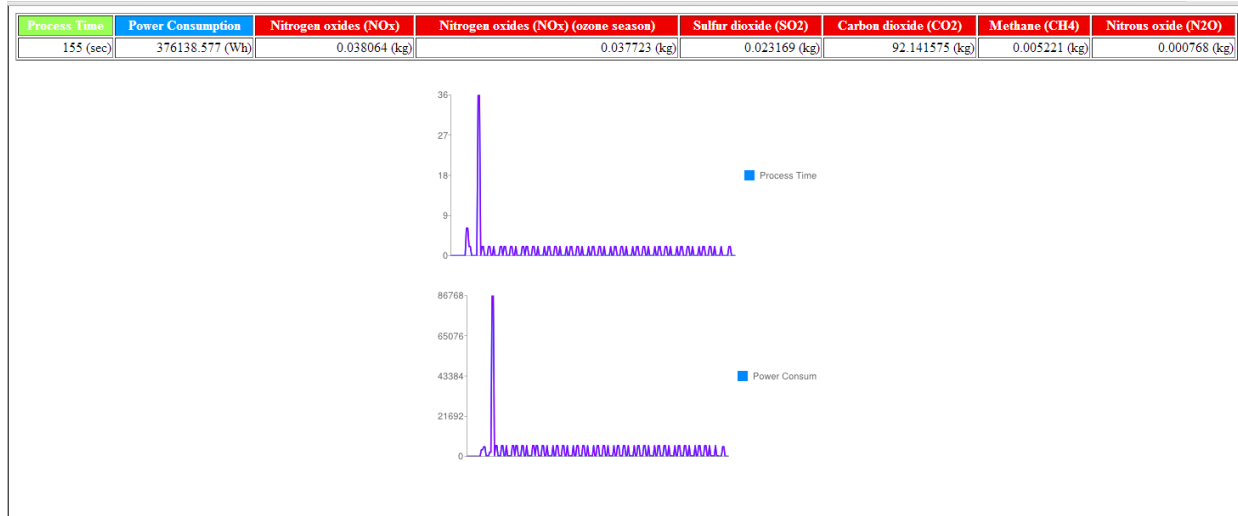


Figure 4.5: The output screen showing the expected time, energy consumption, GHG emissions, and block-by-block plots

used in the trials to compute the customization constants. For example, to compute the customization constants related to the spindle power, $KA_{spindle}$ and $KB_{spindle}$ above, we had used 3000, 4000, and 5000 RPM speeds respectively (Figure 3.4). In the validation trials, we used intermediate speeds of 5500RPM and 6700RPM to corroborate the energy analyzer predictions of $P_{spindle}$ against the measured values. Similarly for movements and cutting, we used different combinations of X and Y direction feeds and depths of cut than those used when computing the customization constants. Results from the two types of validation trials are presented in the next two sub-sections.

4.4.1 Validation of various power states

In the first set of validation trials, we validate the intermediate power states of the CNC machine as predicted by the energy analyzer. In all these trials, we used the “MDI” mode of the CNC machine in order to measure a particular power state. By using MDI mode, it was possible to isolate power consumption easily because unlike a program run, the machine stops after each MDI command. In Table 4.1, the power states predicted by the energy analyzer and those measured by the Yokogawa meter are compared. Deviation from the observed power state values, was within 1-6%.

4.4.2 Validation of complete NC codes (toolpaths)

In the subsequent validation trials, we measured the energy consumption of various complete NC codes (toolpaths) and compared the measured values with those predicted by the energy analyzer. These trials were performed in the (usual) program mode with a

Table 4.1: Validation of power states

Power State	Estimate (W)	Avg. Measured (W) [T1, T2, T3]	Deviation (%)
Constant Power (tare, coolant pump) (P_{const})	325	323 [323, 320, 325]	-0.6
Spindle Power ($P_{spindle}$ at 5500 rpm)	1257	1270 [1290, 1260, 1260]	-1
Spindle Power ($P_{spindle}$ at 6700 rpm)	1526	1540 [1530, 1540, 1550]	-1
X-direction P_{move} , 25% Rapid	296	310 [310, 310, 310]	-4
X-direction P_{move} , 60% Rapid	361	380 [390, 370, 380]	-5
Y-direction P_{move} , 25% Rapid	365	360 [360, 360, 360]	3
Y-direction P_{move} , 60% Rapid	388	400 [390, 400, 410]	-3
X-direction P_{cut} , Feed 30 IPM	314	300 [300, 290, 310]	5
X-direction P_{cut} , Feed 50 IPM	347	370 [370, 370, 370]	-6
Y-direction P_{cut} , Feed 30 IPM	402	430 [420, 440, 430]	-6
Y-direction P_{cut} , Feed 50 IPM	429	440 [460, 430, 430]	-2

Yokogawa CW240 meter connected to the machine to measure the electricity consumption of the complete NC code. Toolpaths used in these validation trials are shown schematically in Figure 4.6. In Table 4.2, results of the validation trials for 6 complete NC codes are presented along with the calculated percentage deviations. Similar to customization constants, each measured power state is an average power state value of the three independent observations in the square brackets.

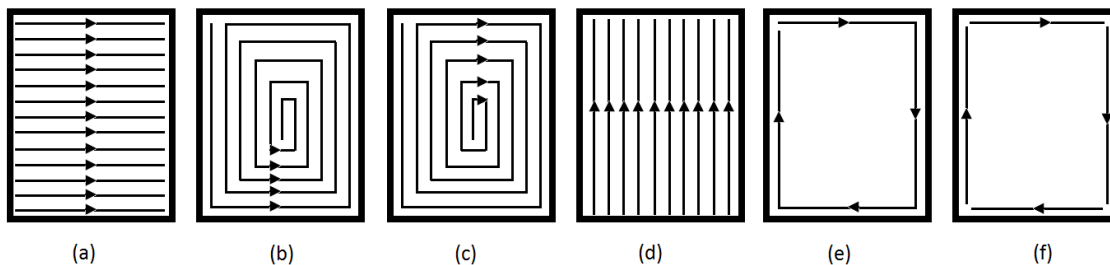


Figure 4.6: (a-f) Schematics of the six toolpaths used in validation checks.

Table 4.2: Validation of NC codes (toolpaths)

	Time (s)		Energy (W-sec)		Deviation (%)	
	Estimated	Measured	Estimated	Measured	Time	Energy
a. Component 1 (Facing, X directional)	286	290	109,876	106,475	-1	3
b. Component 1 (Spiraling in)	262	265	109,223	114,542	-1	-4
c. Component 1 (Spiraling out)	267	280	123,871	130,652	-4	-6
d. Component 1 (Facing, Y directional)	291	287	147,190	142,601	1	3
e. One contour of a face	17.2	17.3	28,407	27,913	0	1
f. Sides of a face contour	15.6	17	28,012	27,633	-2	1

We found that our energy analyzer successfully predicted the time and the energy usage for every toolpath within a range of -6% to +3% and that the trends predicted by the

energy analyzer (e.g. the energy usage of X-directional facing smaller as compared to the Y-directional facing, the energy usage of spiraling in smaller than that of spiraling out) also matched with the observed values in machining trials. The deviation of the estimates from the observed values was found on both sides of the observed values.

We believe that the results of the validation checks are promising and that the energy analyzer can be used with a reasonable faith to estimate time and energy consumption of NC codes without having to actually execute the codes on a CNC machine. We further propose that the energy analyzer can also be used to rank different toolpaths against each other since the trends in the validation checks were consistent with those found in the machining trials.

4.5 Conclusion

In this chapter, we described the development of energy analyzer software based on the energy model we proposed in the previous chapter. The energy analyzer software is readily usable in a browser without the need of any additional software or libraries. Once customized to a target CNC machine using a one-time customization step, the energy analyzer is able to estimate the expected electricity requirements (in W-sec) and the expected machining time (in seconds) for any NC code for the target CNC machine. We also validated the energy analyzer's estimates by several experiments, as shown in Tables 4.1 and 4.2.

We now have a validated software tool to compare and contrast NC codes (e.g. alternative toolpaths for the same component by different strategies) on the basis of their expected energy consumption, without the need of actual cutting. In the following chapter, we demonstrate this real-world use of the energy analyzer with several case studies that compare various toolpath alternatives obtained from commercial CAM software for their energy requirements.

Chapter 5

Energy Analyzer: Examples

We proposed an energy consumption model for 3-axis CNC milling machines in Chapter 3 and described the development and validation of the energy analyzer software tool based on the model in Chapter 4. In this chapter, we describe several case studies to illustrate the use and the importance of the software in practical scenarios. The energy analyzer is meant to be a supportive CAM tool, positioned between the process planning and actual machining stages in manufacturing a part. Thus, in most case studies that we present here, the inputs are components to be machined and NC codes generated for the machining operations using commercial CAM software (Mastercam). We compare the energy and time estimates for different alternative NC codes (toolpaths) of components using the energy analyzer, without actually cutting any of them. Such an estimate-based comparison — currently not possible by any commercial methods or tools — enables process planners to make better-informed process planning decisions without wasting any resources or machine time. As the case studies presented in this chapter indicate, our validated energy analyzer can help identify energy saving opportunities that may otherwise go unnoticed in productivity-oriented (traditional) process planning.

In the first case study, we illustrate the energy analyzer's use to select a toolpath from two seemingly equivalent toolpath alternatives. The two alternative toolpaths, in this case for facing a square block, are identical in almost every sense including the expected machining time. However, significant energy saving potential still exists as it will be seen in the case study. In the second case study, we demonstrate the importance of various geometric aspects of the toolpaths and their effects on energy consumption in machining. In the third case study, too, we compare facing of a similar square block, but with two different toolpath strategies to identify important energy consumption related trends. This chapter leads into the next chapter that identifies important energy consumption trends in CNC machining toolpaths.

5.1 Case study 1: Facing operation alternatives

Objective: In this case study, we use the energy analyzer to compare the energy

requirements of two nearly-identical alternative toolpaths for facing a square block that only differ in the direction of cut.

Procedure: Commercial CAM software programs (e.g. MasterCAM) provide many alternative strategies for facing; we consider the zig-zag machining strategy for this case study, due to its popularity as the strategy of choice in rough machining operations such as facing [Lasemi et al. 2010]. We deliberately generate NC codes from two toolpaths such that other than the primary direction of cut, all other geometric and mechanical parameters of the two toolpaths being compared are identical. Toolpath A, seen in Fig. 5.1a, has the majority of cutting in X-axis parallel direction while toolpath B, seen in Fig. 5.1b, has the majority of cutting in Y-axis parallel direction. Since this case study is for a square block, both toolpath alternatives have nearly identical machining time for the same cutter diameter and overlap. Results from running the energy analyzer for the two toolpaths (using NC codes generated by MasterCAM) are presented side-by-side in Table 5.1.

Observations and inferences: We notice that, although the expected machining time for the two toolpaths is nearly identical (324 vs. 318 seconds), toolpath A, where most of the cutting happens along the X-axis, is estimated to require about 20% less energy than toolpath B, where most of the cutting happens along the Y axis direction. Based on the observations in the previous chapter during power-states validation, we anticipate that due to the differences in axis construction, motor capacities, and the bearing sizes, the amount of energy to move or cut in X-axis direction is more than that in Y-axis direction. Haas VF-0 machine has the X-axis mounted on top of the Y-axis as seen in Figure 5.2. As a result, when machining in Y-axis direction, the whole mass of the X-axis motors, bearings, guides, etc. must move, which may be the reason for the difference in energy requirements of the axes. Both toolpaths require nearly identical machining time (the small difference is due to difference in positioning) due to the square geometry of the face and identical toolpath strategy in both cases.

Table 5.1: Comparison of estimates for facing operation alternatives

Toolpath	Energy (W-s)	Time (s)
X-directional facing	106,241	324
Y-directional facing	130,497	318

Significance: The observed difference in energy consumption for identical movements in different axis directions is remarkable. Figure 5.3 shows a CNC machine used in industry — Heynumill PF 3200. Unlike the Haas VF-0, this much bigger machine has a different axis configuration. Although one is not mounted on the other, the two principal axes can be expected to have significantly different energy consumption properties because one of them carries the additional mass of the spindle and the tool changer magazine (the gantry-styled axis) while the other (the table) carries the additional mass of the work-piece itself (7,500 Kg against 57,000 Kg). Further, the axis motors used to move the axes have power ratings of 9.7 KW against 34.2 KW. Thus, in facing a rectangular face on this machine, machining

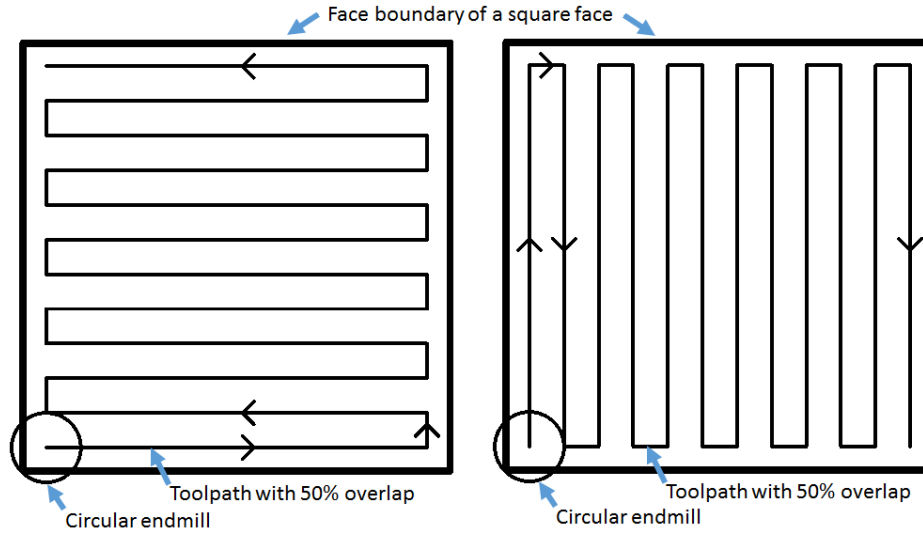


Figure 5.1: Face-milling a square face with cutting primarily in (a) X-axis direction (b) Y-axis direction

along the first direction may be significantly more energy-efficient when compared to facing along the other direction.

5.2 Case study 2: Effect of “corners” in toolpath

Objective: In this case study, we use different toolpath strategies to further focus on the number of corners in a toolpath.

Procedure: We compare the expected energy consumption of two toolpaths alternatives for facing a square block using two entirely different strategies that are popularly used in industry. For facing a square block, in MasterCAM, we select a contour-parallel toolpath and a spiral (inwards) toolpath with the same percentage overlap. The toolpath based on contour-parallel strategy has significantly more 90-degree turns or corners (Figure 5.4a), while the one based on the spiral strategy has virtually no sharp turns Figure 5.4b. The expected machining time (from MasterCAM) for the spiral strategy toolpath is approximately the same as that for the contour-parallel toolpath.

Observations and inferences: Results from running the energy analyzer for the two toolpaths (using NC codes generated by MasterCAM) are presented side-by-side in Table 5.2. We find that the spiral strategy is only slightly efficient in terms of machining time but may save energy (10%) during machining. This behavior may be attributed to frequent and sudden accelerations or deceleration of the axes motors (at corners) that results in higher instantaneous power consumption. [Chen et al. 2009] report that a toolpath with numerous corners, as found in the contour-parallel toolpath in this case-study, may result in tool marks on the machined surface due to sudden acceleration of the axes.

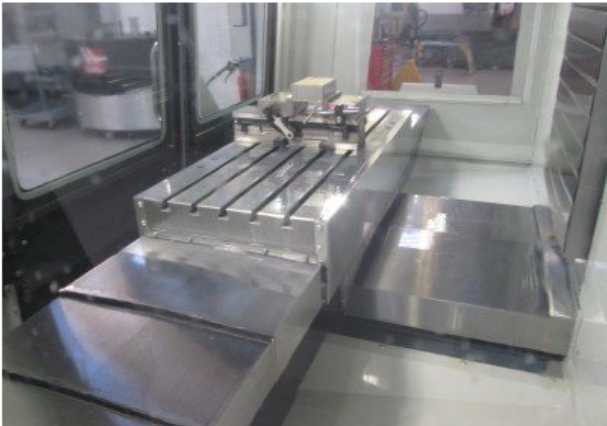
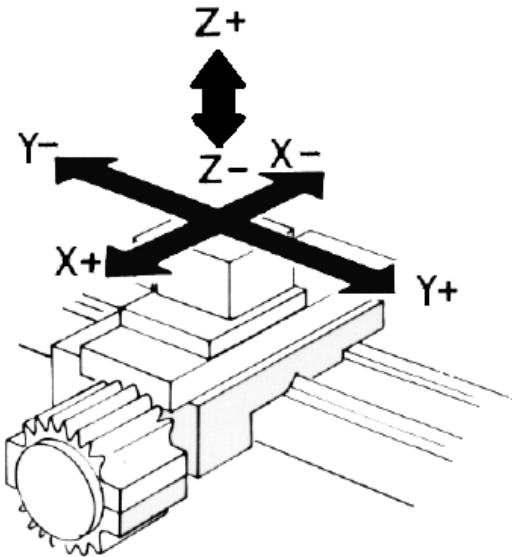


Figure 5.2: Axes mounting in Haas VF-0 indicating X-axis being mounted atop Y-axis

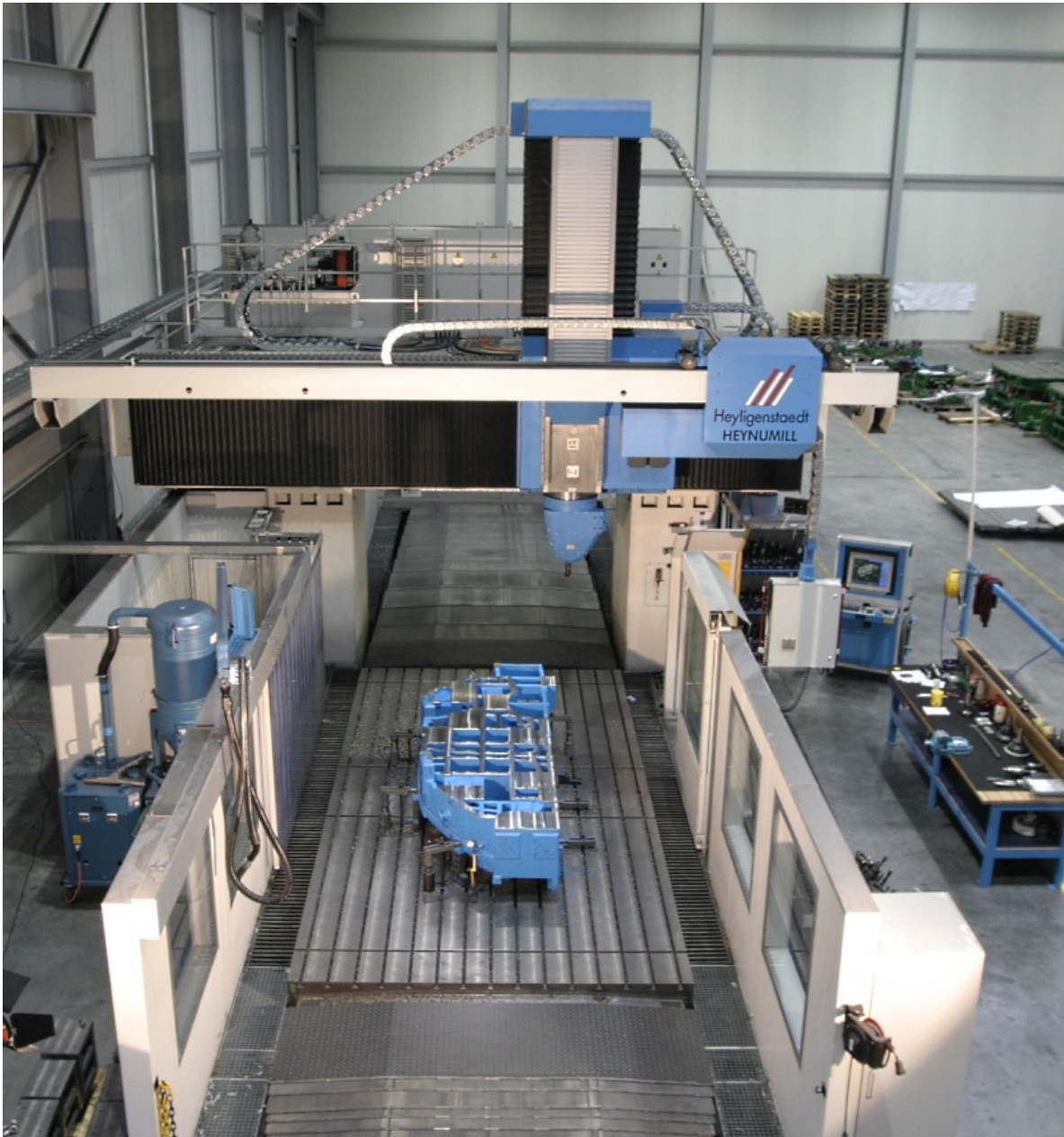


Figure 5.3: An industrial CNC machine used in the automotive industry — the Heynumill 3200 PF

Thus, we can tentatively claim that corners in a toolpath are not favorable for energy efficiency since they represent lost time and energy in starting and stopping an axis motor.

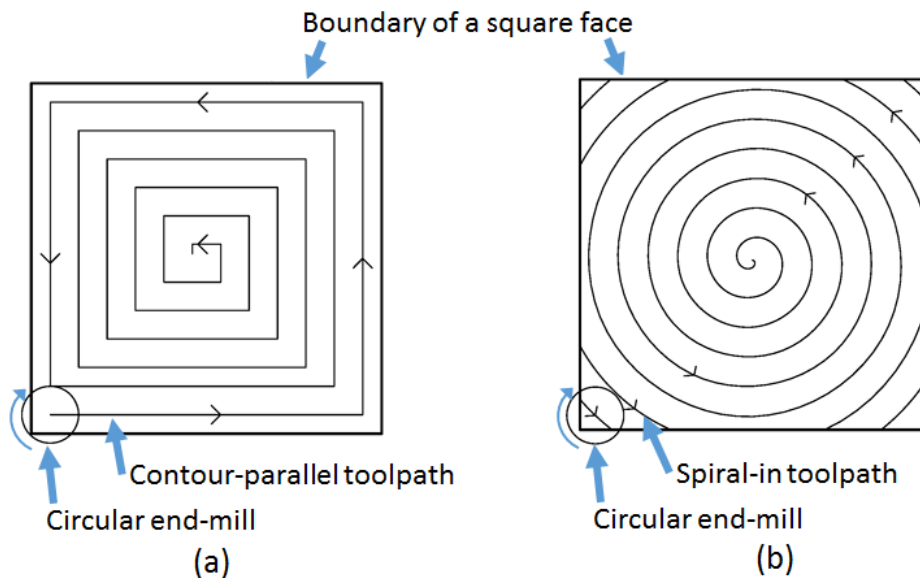


Figure 5.4: (a) Contour-parallel (b) Spiral toolpath for a square facing operation

Table 5.2: Comparison of estimates for spiral and contour parallel toolpaths

Toolpath	Energy (W-s)	Time (s)
Contour-parallel	88,144	234
True spiral	78,896	219

5.3 Case study 3: Effect of input geometry

Objective: In this example, we highlight the importance of input geometry when deciding a strategy for machining. We again compare the same two toolpath strategies (one with and the other without sharp corners) to generate toolpaths a different input face geometry: a rectangular face with two islands.

Procedure: We compare the expected energy consumption of two toolpaths alternatives for facing the input geometry with islands using the same two strategies used in the previous example. We again generate the required toolpaths in MasterCAM, one with a contour-parallel toolpath strategy and the other with a spiral (inwards) toolpath strategy with the same percentage overlap. The toolpath based on contour-parallel strategy

has significantly more 90-degree turns or corners (Figure 5.5a), while the one based on the spiral strategy has virtually no sharp turns but has many lifts resulting from the islands. Figure 5.5b.

Observations and inferences: Results from running the energy analyzer for the two toolpaths (using NC codes generated by MasterCAM) are presented side-by-side in Table 5.3.

Significance: We now find that the spiral strategy is in fact 10% less efficient in terms of machining time and energy consumption as compared to the contour parallel strategy for this input geometry. This is in stark contrast to the earlier example where the spiral strategy was found to be energy efficient as compared to the contour-parallel toolpath strategy. Thus, we find that although corners are worse for energy consumption of a toolpath (from the earlier example), the input geometry also plays an important role in deciding a strategy for machining a component and that no one strategy can be guaranteed to be energy efficient for all input geometries.

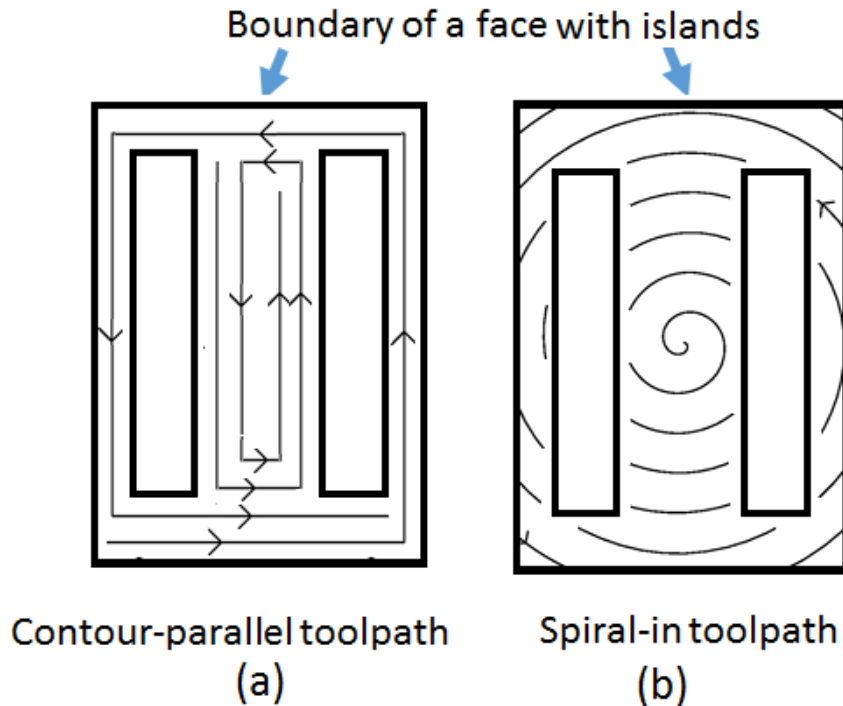


Figure 5.5: (a) Contour-parallel (b) Spiral toolpath for a facing operation for a face with islands

The three cases explained above illustrate possible use-cases for the energy analyzer as a supporting software to MasterCAM or any other toolpath planning software to make decisions aware of the energy costs. Although the analyzer's predictions were validated for

Table 5.3: Comparison of estimates for spiral and contour parallel toolpaths for a face with islands

Toolpath	Energy (W-s)	Time (s)
Contour-parallel	109,874	311
True spiral	121,710	349

both precision and trends (in the previous chapter), we identify here, some of its limitations that arise from the data acquisition process or the equipment available for testing in a university machine shop.

5.4 Energy analyzer limitations

- The time computations in the energy analyzer assume a linear acceleration and deceleration profile of the axis motors. Since we wanted to avoid reliance on machine handbook data during customization, this assumption was necessary to obtain reasonably accurate time estimates. We also use a single, almost universal value of $1m/s^2$ for the acceleration of an axis. These computations can be further improved with more accurate computations based on the actual motor curves and acceleration profiles although it may be difficult to practically determine these without using the machine handbook data with a low-frequency energy meter like a Yokogawa CW240. Similarly, the peak corresponding to the spindle start may also be taken into account in time and energy estimations if its duration and height can be accurately measured.
- The energy estimates in the energy analyzer are based on an inherent assumption that up-milling and down-milling¹ require the same amount of energy if all other conditions are identical. This, however, is only an approximation. Theoretically, down-milling requires less energy due to the geometry of cutting forces that tend to force the workpiece into the table. We investigated this factor during our experimentation but could not get a clear trend to confirm the difference in power consumption when up- or down-milling happens. Also, with only NC code of an operation as the input, it is impossible to know if a block of NC code will cause up- or down- milling. Therefore, we have not included this factor in the analysis when computing the energy usage. However, in future, energy analyzer can be improved if up/down milling is separately considered, perhaps as an additional user input factor.
- [Avram and Xirouchakis 2011] recommend that in order to identify stable cutting conditions when measuring energy consumption by a CNC machine, a modal analysis must be performed. Based on the frequency response function of the machine tool, stability lobe diagrams should be developed using to ensure that during the acquisition,

¹Refer to [CNC Cookbook 2014] for definitions

no oscillation behavior or any other undesired effects occur that may affect the measured electric signals of voltage and current.

- The data acquisition process suffers from fluctuations in power supply, effects due to the presence of other electric equipment in the vicinity, and the relatively lower frequency of measurement of the energy meter – Yokogawa CW240 (10Hz). Ideally, the energy meter must be integrated with the CNC controller such that energy usage per block is measured and recorded individually. A meter with higher frequency of measurement may be necessary for more accurate measurements, particularly if the measurement signals will be used for online monitoring of machining conditions [Vijayaraghavan and Dornfeld 2010]. A WattNode energy meter [Continental Control Systems 2009-2014] may be suitable for this purpose but using a Wattnode meter requires special dedicated wiring setup that may be difficult to perform on a machine regularly used in an industry.

5.5 Summary

The objective of the energy analyzer is to provide a means to compare various alternative toolpaths for a machining task based on expected energy consumption specific to candidate machine construction, process conditions, and the geometric parameters of the toolpaths. The analyzer uses our analytical process model for CNC milling tuned to the specific machine in question by brief customization trials. To our knowledge, no such machine-specific, validated comparison software exists today to consider environmental aspects in toolpath planning for CNC milling. As we demonstrated, even with the current limitations, the energy analyzer has immediate practical applications in industry since it may be used along with any existing CAM/toolpath planning software, without making any other changes to the machine or the workpiece design, for tangible energy savings by merely operating the machines differently and selecting toolpaths based on their expected energy consumption.

Extending the discussion on saving energy in CNC machining, in the next chapter, we explore a more proactive approach to toolpath planning by generating new toolpaths (as opposed to the reactive approach of selecting toolpaths from available alternatives) that are designed to consume less energy for the same task.

Chapter 6

Toward Energy Efficient Toolpaths

In the previous chapter, we demonstrated three real-life example cases where possible use of our energy analyzer (described in Chapter 4) was demonstrated in CNC process planning to make decisions aware of the impacts on energy consumption. In this chapter, we develop additional knowledge and tools to progress a step further by designing manufacturing processes such that they are inherently energy-efficient. We first enlist important characteristics of NC codes/toolpaths that affect energy consumption in CNC machining followed by the description of a novel method of designing inherently energy-efficient toolpaths.

6.1 Factors Affecting Energy Consumption

We analyzed several different NC toolpaths for a variety of workpiece geometries, both by using the energy analyzer and by observing the actual energy consumption using a Yokogawa CW240 energy meter. We observed the following characteristics of toolpaths, underlying toolpath strategies, toolpath parameters, and machining conditions that prominently affected energy consumption in machining.

1. Strategy: We found that no single toolpath strategy (topology) may be universally adapted as “the most energy-efficient” strategy to follow when generating toolpaths for 3-axis CNC milling. For instance, a true-spiral strategy in MasterCAM was generally found to be the most time and energy efficient for non-rectangular, circular or oval pockets but the same strategy failed when there the inputs were rectangular or had slender islands. Instead, we believe that the energy consumption depends may vary by the machine, the workpiece geometry, and also the electrical characteristics of various machine components (e.g. axis motors).
2. Direction: Further, even the same toolpath strategy (topology), when used in different primary directions, may result in different energy consumption, because a machine may require a different amount of energy to move/cut in different directions. For example,

in the Haas VF-0 3-axis CNC milling machine, the X axis is physically mounted on top of the Y-axis, resulting in a higher power requirement when cutting or moving along the Y-axis, due to the additional mass of the X-axis that must also move every time the Y-axis moves. Thus even for the same strategy, a different amount of energy is required when cutting is done along the X-axis versus along the Y-axis.

3. Machine variability: In addition to not finding a single most effective strategy or direction, as [Balogun et al. 2013]’s findings suggest, the relative performance of various toolpaths can too change from machine to machine since machine construction, axis mounting, etc. may differ. In other words, a toolpath found to be the most efficient among available alternative toolpaths on Haas VF-0 may or may not be the most efficient when the same candidate toolpaths are analyzed for a different machine with different customization constants.

However, we also found several geometric characteristics of toolpaths that tend to result in lower energy consumption irrespective of the underlying strategy or cutting direction. We found that:

1. A toolpath that makes fewer and gradual changes in cutting direction is better for reduced energy consumption. Extensive and frequent changes in tool-path direction are unfavorable since they cause spikes in the power demand resulting in higher overall energy consumption in the process. [Lasemi et al. 2010] have also reported that such sudden acceleration events (jerks) reduce the tool life due to fatigue.
2. Toolpaths that avoid sharp corners and frequent lifts tend to reduce the machining time and energy consumed. Toolpaths with continuously varying, low curvature (without sharp corners or turns), avoid repeated acceleration/deceleration events that cause spikes in power consumption. Also, frequently lifting and repositioning the tool results in air-cutting causing higher cycle time and energy requirement.
3. Maintaining constant cutting loads by using longer segments with near constant machining rate results in lower energy consumption. Additionally, these paths are also favorable for surface finish and tool life.
4. Direction of tool-paths: Wisely choosing the direction to obtain longer paths also help in significantly reducing the cutting time, and as a result, saving energy. Thus, fewer long cutting paths in one direction are better than many short paths.

Based on the above observations, we anticipate that toolpath planning for energy efficient machine may involve some trade-offs. For example, for lower energy machining, a larger percentage overlap between two adjacent toolpath segments would be detrimental due to increased number of toolpath segments for the same component. But, a higher overlap is better if superior surface-finish is also desired after machining. Thus, the toolpath planning strategy or topology and the process planning software must optimize a weighted combination

of possibly contradictory objectives. Therefore, we cannot recommend any one strategy or technique among existing strategies offered by commercial CAM software (e.g. Espirit, MasterCAM) that could be used to generate toolpaths that will be both productive and energy-efficient by design.

We were introduced to a research work by [Maharik et al. 2011] in the domain of computational art that we found inspiring as a foundation to develop toolpaths that will be energy-efficient by design. The next section describes this work briefly; for a more complete account of the work, the reader is referred to the original publication [Maharik et al. 2011].

6.2 Digital micrography

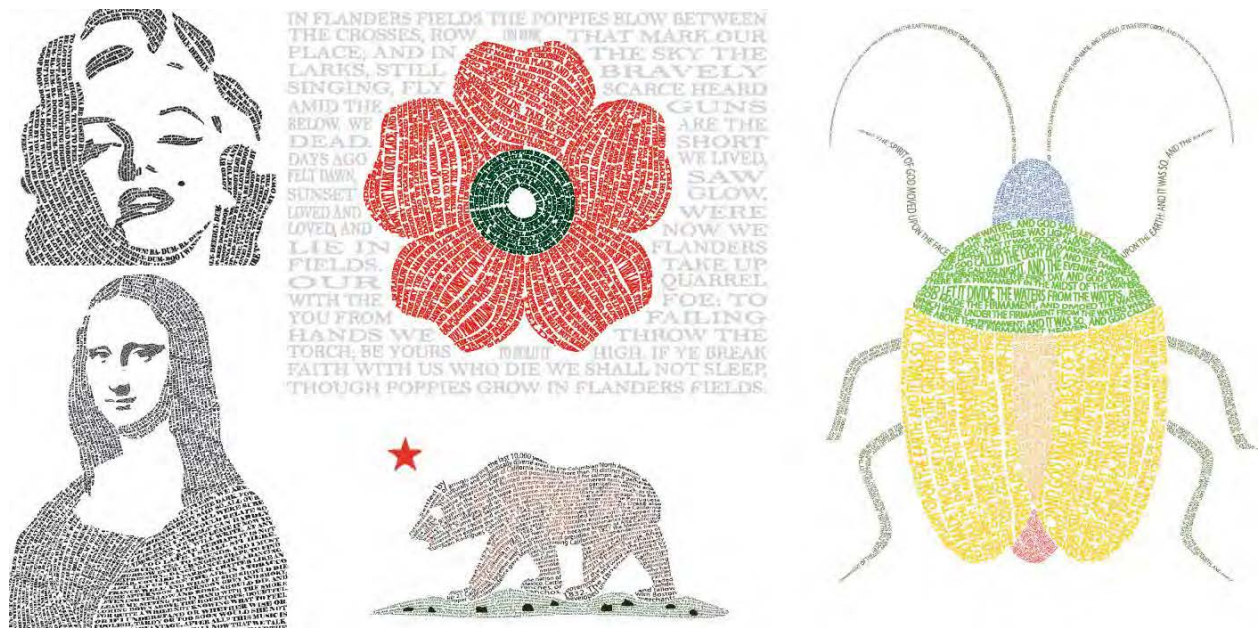


Figure 6.1: Examples of micrographic text arrangements as reported in [Maharik et al. 2011]

The digital micrography technique focuses on generating aesthetically pleasing text arrangements that convey an underlying 2D shape while still being readable. Micrographic text arrangements, as shown in Figure 6.1, are a special type of calligraphic arrangement of text. These are highly artistic arrangements of text that can take hours to create manually. Maharik et al. generate complex micrographic arrangements automatically, by developing an algorithm to automatically place the text.

Automatic generation of micrographic images starts with designing a smooth vector-field over the input geometry, followed by tracing streamlines that act as seed points to place text. Once streamlines are traced from the designed vector-field, text is placed and re-sized along the streamlines to generate the final output. This process is shown for an example shape in Figure 6.2.

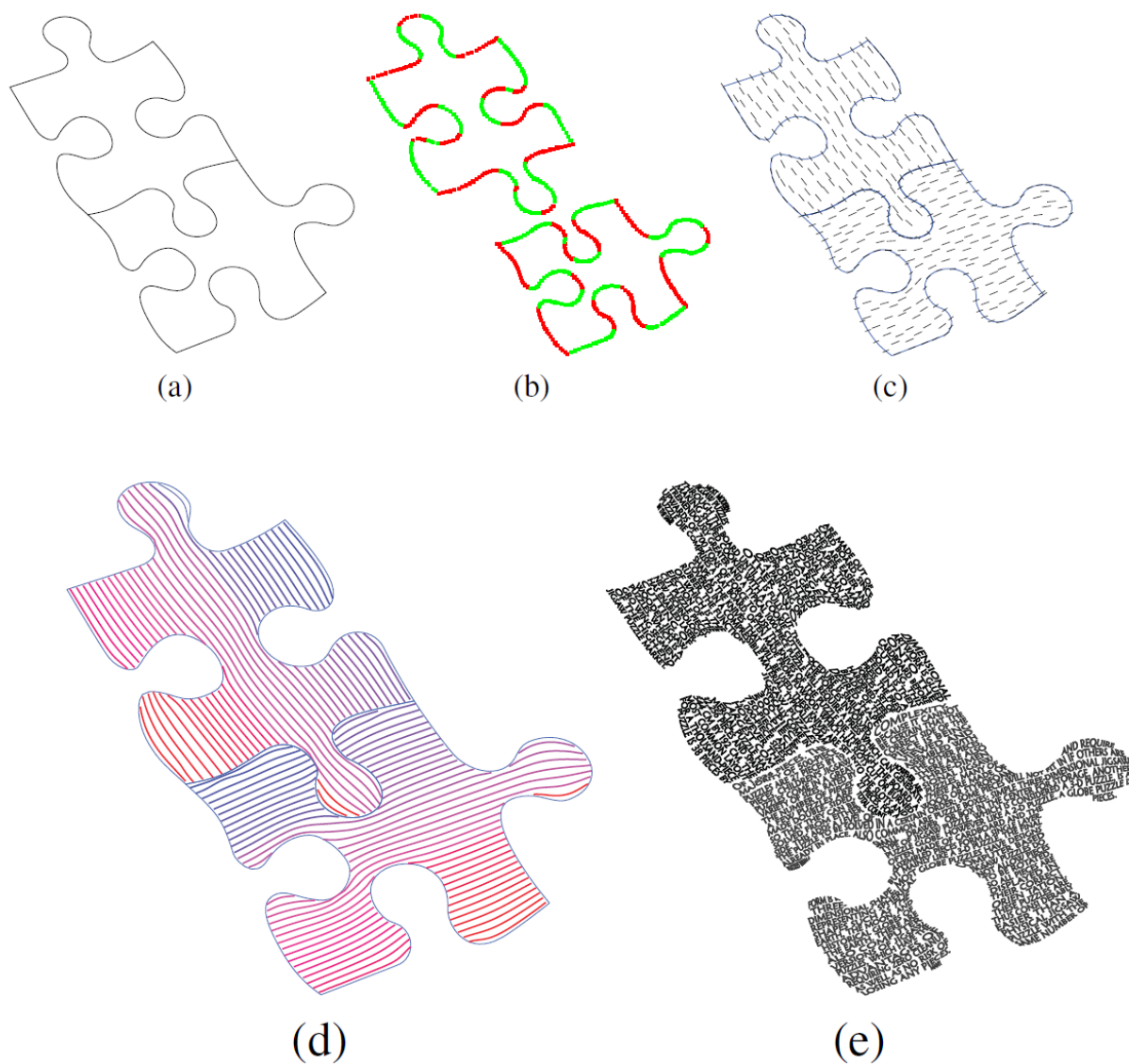


Figure 6.2: (a) Starting 2D geometry, (b) boundary conditions for a desired vector field, (c) a suitable vector field that satisfies the set boundary conditions, (d) tracing vector-field streamlines, orienting and ordering them, and (e) placing text along the streamlines. [Maharik et al. 2011]

Maharik et al. focused on two principal requirements when generating digital micrographic images: shape recognition and readability of the text. First, for shape recognition and aesthetic appeal of micrographic figures, the text conforms to the outline shape. Also, since the text layout defines the outline of the shape, the text line directions are aligned with the image region boundaries when possible. Specifically, acute angles between boundaries and text directions are avoided. The text is placed in lines with low curvature, high coherency, and such that adjacent lines are equi-spaced. Such lines are important not only for readability but also for visual appeal. Further, for readability, uniform, left to right text flow is maintained to help the reader follow the lines of text easily. The lines have low curvature with no sharp changes in direction. They also have as much length as possible. Based on these requirements and the trends we identified in section 6.1 above, we postulated that the underlying technique in generating micrographic images can be extended into a toolpath strategy (similar to zig-zag or contour-parallel strategies) for generating toolpaths that inherently have properties of energy efficient toolpaths. This idea led us to our final case study.

6.3 Towards inherently energy efficient toolpaths

We explored the idea of using a micrography-like process to generate 3-axis CNC milling toolpaths because we found that the underlying problems in both toolpath planning and digital micrography had some distinct commonalities. Our colleagues in the Computer Aided Design and Manufacturing Laboratory at UC Berkeley (Youngwook Kwon, Sushrut Pande, and Zhongyin Hu) worked on connecting the streamlines (from digital micrography process) and generating an NC code (toolpath) using points on the streamlines as cutter location points for an input shape — the bear, shown in Fig. 6.1(center-bottom) — also used in the digital micrography paper. The streamlines and the input geometry were kindly made available by the digital micrography research team. For this dissertation, we compare the energy performance of this micrography-inspired toolpath with an equivalent toolpath obtained from MasterCAM.

MasterCAM provides several alternative pocketing strategies (shown in Figure 6.4). Although it is difficult to select an equivalent toolpath to compare against that obtained from digital micrography, we decided to fix the depth of the pocket and select a MasterCAM alternative toolpath that removed the planned material — the bear shape, 0.025inch deep — in the least amount of time. Thus, in essence, we compared the most time-efficient MasterCAM toolpath for the same amount of material removed (the most resultant MRR) against the toolpath based on digital micrography. We compared the time estimates made by MasterCAM to compare its alternatives (see Table 6.1) and found that the X-parallel one-way toolpath was the most time-efficient toolpath among the available alternatives to compare against the novel, micrography-based toolpath. In this comparison, we ignored the high-speed machining toolpath provided by MasterCAM because although it had the least expected machining time, it did not result in complete machining of the component.



Figure 6.3: Starting 2D geometry

The objective of this case study was two fold: (a) we wanted to test the energy analyzer on two real-world toolpaths to validate the accuracy of its estimates; (b) we wanted to test if micrography-based toolpaths were indeed energy-efficient when compared to MasterCAM generated, commonly used toolpaths. Even for the same machining time and the same material removed (hence the same MRR), we wanted to know if the followed path had any effect on the energy consumption.

Table 6.1: Comparison of MasterCAM’s time estimates for the 6 toolpath alternatives.

Toolpath strategy	Estimated machining time	Remarks
(A) Constant overlap spiral	32 min. 01 sec.	
(B) One way, X parallel	30 min. 16 sec.	The least time
(C) Parallel spiral	34 min. 27 sec.	
(D) One way, Y parallel	47 min. 30 sec.	
(E) True spiral	105 min. 01 sec.	
(F) High speed machining	29 min. 12 sec.	Some material left

6.3.1 Setup and toolpath generation

Since this trial is focused on comparing the energy performance of the two toolpaths, we made a conscious effort to keep most other parameters identical for a fair comparison. We use the same input geometry to generate both — micrography-based and MasterCAM — toolpaths, use the same workpiece material (Aluminum 6061 alloy) and cutter (3/32 inch, 2-flute, uncoated flat end-mill), and use the same CNC machine for our trials. As previously described, we selected a toolpath from MasterCAM alternatives that required

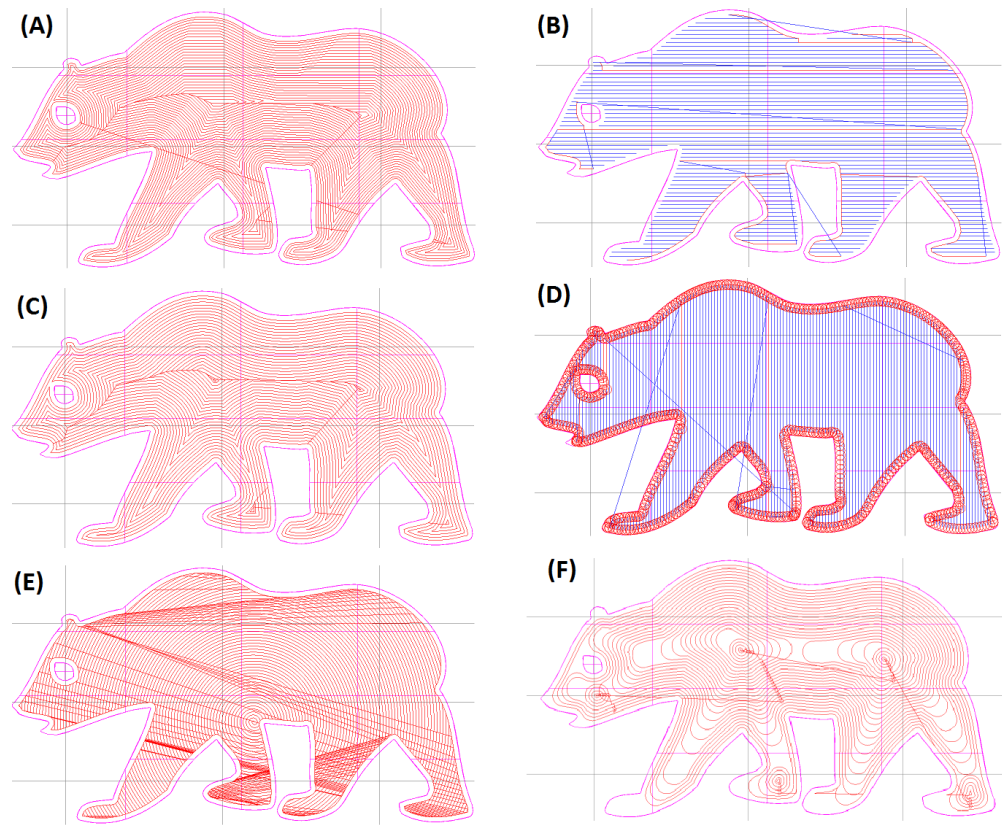


Figure 6.4: 6 alternative strategies from MasterCAM (A) Constant overlap spiral (B) One-way, X-parallel (C) Parallel spiral (D) One-way, Y-parallel (E) True spiral (F) High-speed machining

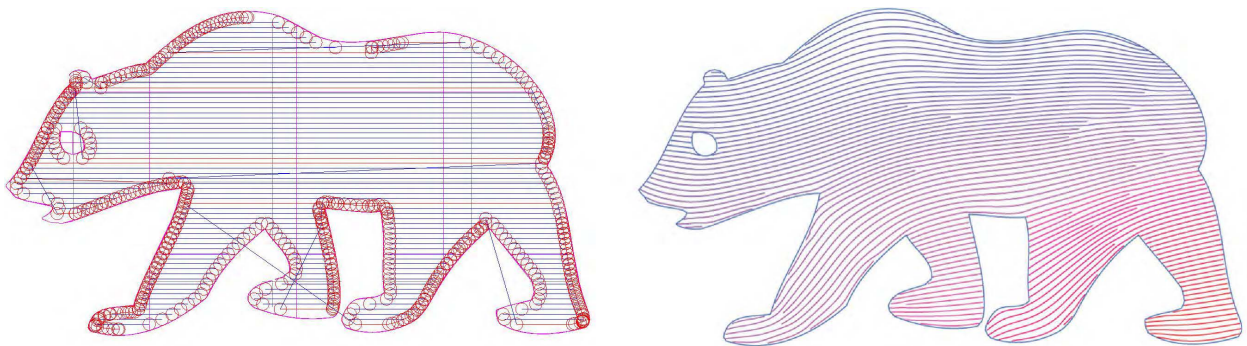


Figure 6.5: Schematic toolpaths for the bear component: (left) using direction-parallel strategy in MasterCAM and (right) streamlines generated in digital micrography research that were connected and used as a toolpath. For connecting, Sushrut Pande developed and implemented an algorithm that is reported in [Pande et al. 2013].

the least machining time and performed complete machining of the component. The input geometry is shown in Figure 6.3, the schematics of the two toolpaths are shown side-by-side in Figure 6.5, while photographs of the two components, after de-burring, are shown in Figure 6.6. The resultant cycle times and energy requirements by both the energy analyzer and as measured are shown in Table 6.2.



Figure 6.6: Schematic toolpaths for the bear component: (left) using direction-parallel strategy in MasterCAM and (right) using the streamlines generated in digital micrography research.

6.3.2 Results

Table 6.2 validates reasonable accuracy of the energy analyzer estimates and, more importantly, indicates that a toolpath generated using principles of energy efficient toolpaths did in fact result in a toolpath that consumed less electricity than a commercial software-generated toolpath for the same of material removal rate. The results also suggest that generating toolpaths by using points on streamlines from the research on digital micrography is a feasible method for generating toolpaths with inherent energy efficient characteristics. We understand that this is only an encouraging start and many further experiments will be needed before guaranteed inherently energy efficient toolpaths can be generated. In the final chapter of this dissertation, we comment on various other research opportunities that can be explored to further the ideas of customized, energy-efficient toolpaths.

Table 6.2: Comparison of time and energy estimates by our energy analyzer with the measured values for the “bear” component.

	Time (s)		Energy (W-sec)	
	Estimated	Measured	Estimated	Measured
Micrography-based	1,480	1,517	2,294,847	2,449,048
X-parallel (MasterCAM)	1,788	1,827	2,618,749	2,893,665

6.4 Summary

In this chapter, learning from various case studies on CAM software-generated toolpaths using different toolpath strategies, process parameters, and machining conditions, we identified important characteristics that make a particular machining operation energy efficient. Professor Alla Sheffer from UBC, who guided a different research on digital micrography first proposed that a portion of their research may be suitably extended for use in toolpath planning. We further identified similarities in the two underlying problems (digital micrography and energy-efficient toolpath generation) to propose generation of toolpaths based on streamlines that could be energy-efficient by design. We tested this hypothesis by analyzing a toolpath generated by our colleagues in our lab using our energy analyzer to find that the toolpath generated using principles from digital micrography consumed about 20% less energy than a toolpath generated using a commercial CAM software for the same machining time. Although more research is required before generation of energy-efficient toolpaths based on the principles of digital micrography can be commercially viable; we believe that these results can convince researchers that in addition to the toolpath strategy and MRR, the workpiece geometry and the intended machine's construction must also be considered when generating toolpaths.

This chapter concludes the discussion of the energy efficiency aspects of 3-axis CNC machining toolpaths. We now shift our focus to the other class of multi-axis CNC machines, where, as explained in Chapter 1, saving energy by reducing the overall cycle time (as compared to saving energy in material removal process alone) may have a larger overall impact due to the energy distribution.

Chapter 7

Toolpath planning for efficiency in 5-axis CNC machining

7.1 Introduction

In line with the objectives of this dissertation to analyze and reduce energy consumption in CNC milling, in this chapter, we report our work on improving energy efficiency in 5-axis CNC milling. Specifically, in the case of 5-axis machining (Section 2.4), reducing operation time by improved toolpath planning may have the most impact on energy consumption. Although toolpath planning for 5-axis machining is a well-researched problem, it is also well-acknowledged that a truly optimal solution to this complex, multi-dimensional problem is yet to be found [Wang and Tang 2007, Farouki and Li 2013].

5-axis CNC machine tools have three translational and two rotational degrees of freedom (DOFs). It is due to the inherent complexity in even formulating a problem that simultaneously accounts for all five DOFs, with multiple, possibly conflicting performance parameters, that researchers separate the DOFs to only formulate and solve a part of the full problem. Two major sub-problems result due to this separation: the toolpath planning sub-problem solves only for translational DOFs, while the tool orientation planning sub-problem only solves for rotational DOFs. Such a separation of DOFs is only a compromise to make the problem tractable when ideally the two interdependent sub-problems should be solved simultaneously.

In this chapter, we propose a novel unified approach to formulate and solve the complete 5-axis toolpath planning problem. Our objective is not to propose yet another method to solve one of the two sub-problems; instead, we want to take on the task of formulating the complete 5-axis toolpath planning problem in a general form that can encompass all current and future aspects (objectives and constraints) of the 5-DOF problem without separating any DOFs in the process. In this chapter, we will:

1. present our proposed formulation of the full 5-axis toolpath planning problem based configuration space (C-space);

2. explain nuances in defining, transforming, and solving the proposed C-space based formulation; and,
3. as a first step toward solving the full 5-axis problem using the proposed formulation, demonstrate the use of this proposed formulation and solution method by applying them to a lower-dimensional problem.

7.2 Past work

Table 2.1 summarizes the past research on 5-axis toolpath planning, which consists of a rich variety of approaches to each of the two sub-problems. The initial research in this area merely aimed at generating a gouge-free toolpath or tool orientations. Many recent works, however, have simultaneously improved performance aspects of the machining process such as the machining time or the surface finish. All approaches presented in the table address only one of the two sub-problems in an independent setting, without solving the other sub-problem simultaneously. However, as we showed in Section 2.4.1, the two sub-problems are inter-dependent and must be solved simultaneously for a truly optimal solution. Some recent approaches can be seen in this direction, as discussed next.

7.2.1 Beyond independent sub-problem solutions

Some recent research works approach the two sub-problems together, albeit with limited scope. [Farouki and Li 2013] solve for tool orientations and toolpath parameters simultaneously to optimize material removal while minimizing angular changes. Although restricted to open surfaces and pre-defined CL paths, this approach computes tool orientations and spacing between CL points simultaneously. [Barakchi Fard and Feng 2009] reported a method with the objective of maximizing machining strip width that considers tool orientations and feed direction computation simultaneously. This approach too, does not consider global gouging but has the important distinction of computing the orientations without fixing the CL points a priori. [Li and Feng 2004] generated iso-scallop toolpaths and tool orientations simultaneously while maximizing material removal; their approach too, however, is restricted to only local gouging checks.

These works not only highlight the importance of solving the sub-problems simultaneously, but also demonstrate the inherent complexity to be expected in formulating such a unified problem. In practice, nearly all components manufactured on 5-axis CNC machines require explicit global gouging checks to avoid tool-workpiece collisions. Hence, to obtain feasible toolpaths, an approach must include checks for local, rear, and global gouging at every CL point. Further, multiple, often contradictory objectives must be simultaneously considered when selecting an optimal toolpath from all feasible alternatives. The recent approaches mentioned above, although a significant advance toward obtaining an optimal solution to the complete problem, are still limited and lack the ability to incorporate multiple objectives. Our formulation in the next sections is based on the idea of optimization since in

our opinion, that framework is the most suitable way to include multiple objectives (material removal rate, machining time, etc.), multiple constraints (gouge-avoidance, acceleration limits, etc.), and multiple DOFs (5 DOFs of the cutter at every CL point) under a single umbrella problem.

7.3 Unified formulation

We recognize that the fundamental objective of the two sub-problems of finding toolpath (CL) points and tool orientations is to completely and correctly machine the workpiece to obtain the design surface. Additionally, due to economical and ecological constraints, the machining process must also be optimized for its performance and environmental footprint. Performance of a machining process is indicated by several parameters such as cycle time, cost, and tool life, while the environmental footprint is characterized by its energy use, emissions, coolant use, etc. The common constraints include those due to gouging prevention, scallop height limit, and kinematic limits. We exploit these similarities in the sub-problem objectives and constraints by expressing them as those of a single optimization problem. Also, we define the optimization problem in the combined parameter space, which is the full configuration space (C-space) [Lozano-Perez 1983] of the cutter. We define this “unified” C-space based problem formulation as follows.

7.3.1 C-space based problem formulation

We formulate the problem by transforming it from a CL path planning/orientation computation to a multi-objective optimization problem where all objectives (e.g. minimizing machining time, maximizing surface quality, etc.) are considered together simultaneously, subject to various imposed constraints expressed as variable bounds or non-linear relations. The formulation does not limit the ability to consider either additional objectives or additional constraints, so any number of objectives or constraints can be added as desired. Optimization is then performed in the machining configuration space (C-space), which is a multi-dimensional “parameter space” spanned by the five axes representing the five DOFs of the CNC machine. We achieve this problem transformation as follows:

1. C-space and parameters: The “control variables” in the optimization problem are DOFs of the cutter: three CL point coordinates and two orientation angles. Thus the parameter space, i.e. the C-space, is five dimensional, where each point represents a unique cutter configuration consisting of a CL position $[x, y, z]$ and orientation $[\theta, \phi]$. Consequently, a toolpath is represented as an ordered sequence of 5D points in the C-space.
2. Constraints: “Constraints” (or “obstacles”) are the regions of C-space where configurations cannot exist if they are to be feasible. In CNC machining, every toolpath must ensure that gouging does not happen, that the complete surface is machined within

the specified scallop height, the tool orientation change is limited, and that kinematic limits of the machine tool are never exceeded, etc. Therefore, we identify and remove portions of the C-space (obstacles) that correspond to each of these conditions, before searching for a solution toolpath. Any “feasible” toolpath solution must lie completely outside of all the obstacles.

3. Objective function and optimization: An “objective function” facilitates ranking and comparison of toolpaths during search for optimal solution from all feasible solutions. The solution to the 5-axis toolpath planning problem must optimize the machinist’s objectives such as minimizing machining time or maximizing surface quality, etc. Thus, in the transformed problem, we define the objective function as a function of configurations — summed over a toolpath — consisting of weighted scores that determine the toolpath’s performance with respect to each objective. The scores result from choices of configurations present in the toolpath; therefore mathematically minimizing the objective function results in a toolpath containing the set of configurations that are optimal for the machinist’s objective.

Formally, for a d axis machine tool, we define a toolpath T as an ordered set of n configurations, where each configuration c_j is a d -tuple. To obtain the optimal toolpath:

$$\begin{aligned} \text{Minimize } \bar{g} &= \sum_{i \in \text{Metrics}} (w_i \cdot f_i(T)) \\ \text{where } T &= \{c_1, c_2, c_3, \dots, c_n\}, \\ \text{subject to constraints : } &c_j \in C^d; \quad c_j \notin B^d; \quad f_i(T) \geq S_k \end{aligned}$$

where w_i is the weight assigned to performance metric i , f_i is the scoring function to characterize the performance of a toolpath for the i th performance metric, for example, a cumulative sum of absolute angular orientation change between successive CL points $f_\theta(T) = \sum_T (c_{n,\theta} - c_{n-1,\theta})$; C^d is the full d -dimensional C-space, B^d ($B^d \subseteq C^d$) are the obstacles (regions on the configurations space representing infeasible configurations) in the full C-space, and S_k s are various hard constraints on the performance of candidate toolpaths (e.g. the maximum resultant scallop height for a toolpath candidate).

7.3.2 Optimization search

The above transformation to an optimization problem needs a flexible solution strategy to solve the resultant 5D optimization problem because the problem’s nature may differ depending on objective and constraint function definitions. Generally, the nature of the objective function (e.g. linear vs. non-linear, single vs. multi-objective) helps in determining the mathematical technique that can be used in its solution. However, due to the flexible definition of the objective function, we cannot guarantee even basic mathematical properties (such as differentiability or continuity) of the objective function. In addition, the constraints

will typically include non-linear inequalities; for example, to maintain scallops less than a fixed height, non-linear constraints relating consecutive configurations in a toolpath are necessary. In addition, the higher dimensional C-space C^d itself may or may not be continuous due to the obstacles B^d . Finally, machining complex industrial components will require numerous (thousands or millions) of CC/CL points, although it can be seen that the computations involved are highly parallelizable. Therefore, we must devise an optimization strategy that can optimize linear or non-linear functions, with possibly non-linear constraints, in higher dimensional discontinuous parameter space and preferably manage the computations by parallelizing. The appropriate technique, thus, may be selected depending on the specifics of the problem.

We now present one example problem — from formulation through solution — to illustrate the application of the proposed formulation and solution technique.

7.4 Example implementation

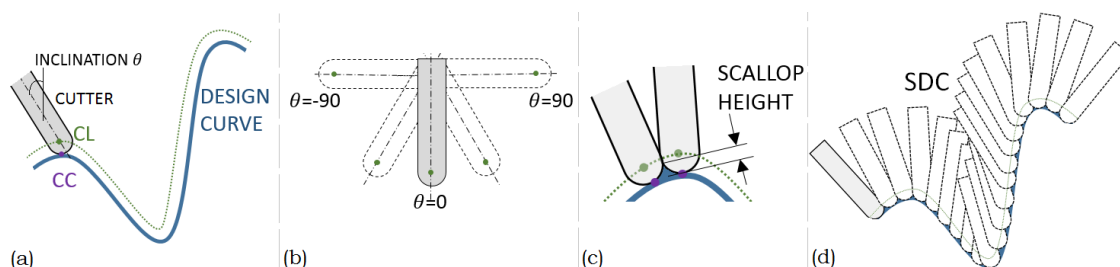


Figure 7.1: Lower dimensional problem setup: (a) design curve and cutter; (b) range of possible cutter orientations; (c) scallop height; (d) resulting surface after “machining.”

Our formulation and solution technique requires geometric computations in higher dimensional parameter space. 5-axis toolpath planning will require a 5D C-space that is difficult to imagine or visualize. As a first step, in the current work we construct and solve a lower dimensional analog of the full problem by artificially reducing the dimensionality. Unlike in the classic work of Lozano-Perez [Lozano-Perez 1983], wherein he discusses a similarly reduced-degree problem for robotic path planning in the plane—a lower-dimensional problem that itself had real-world applications—our lower dimensional problem has no practical application. However, we intend to learn key aspects of the problem’s behavior and the relationship of various inputs to the final toolpaths by being able to easily visualize the C-space and solutions. Thus, our two primary intentions in designing the lower dimensional problem are:

- to provide a proof of concept of our formulation and solution strategy that considers translational and rotational DOFs simultaneously, and

- to facilitate visualization of the C-space and candidate solutions to help learn more about the inherent characteristics of the toolpath planning problem.

We must retain key traits of the full problem (including considering both rotational and translational DOFs) but reduce the computational complexity (dimensionality) when designing the lower-dimensional problem. Also, we should not relax important constraints that may seem redundant in lower dimensions. For example, scallop height is an important consideration, but scallops can occur only when machining a 3D surface and do not arise when machining a single pass with a connected toolpath in lower dimensions. We must avoid losing such constraints while reducing the dimensionality.

We have designed the lower-dimensional problem for this work with the following inputs and assumptions:

- Design surface: A planar parametric curve (Fig. 7.1(a)) that must be obtained.
- Maximum scallop height: Scallops after machining cannot be larger than s units high.
- Cutter: A planar, sufficiently long, ball-nose (semi-circle nose) cutter of radius ρ , that can translate and rotate in the plane. The cutter’s vertical orientation is denoted by orientation $\theta = 0$ and the cutter can be rotated to any angle between -90° to $+90^\circ$ as shown in Fig. 7.1(b).
- “Machining:” Since a connected machining pass in 2D won’t result in scallops, we define the “machining” process plan by a set of discrete configurations (SDC) that we define as a set of CL positions and orientations where the cutter will be placed (and removed), resulting in the final “machined” curve with scallops as shown in Fig. 7.1(d).
- Objective: The objective in this problem is to generate a SDC that results in lower cutting time, higher material removal, and maintains scallops below the set limit subject to the constraints due to gouging. Thus, the objective is defined as a weighted average of individual objectives of cutting time and material removal, where the weights can change according to user preference.

We first construct the full C-space for this problem, obtain the feasible C-space by removing obstacles arising from the constraints, and then perform a search for the optimal SDC.

Constructing the C-space

We construct the C-space using geometric characteristics of the problem and subtract obstacles from it to obtain the feasible C-space. Since in point-milling, the 2D cutter may touch the parametric design curve only at a single point (CC), there exists a unique CL point for each CC point on the curve. Thus, each CL point can be identified by a unique parameter value of the design curve. Thus, we can treat the two in-plane translational

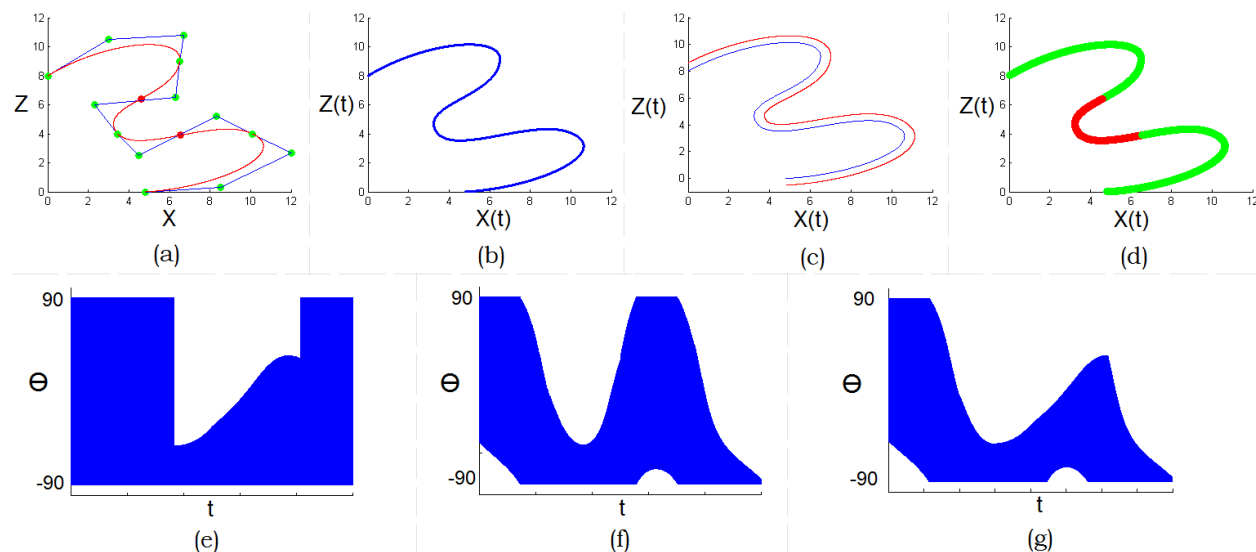


Figure 7.2: Solving the lower-dimensional variant. (a) The design curve to be machined and its Bezier control points. (b) Evaluated design curve points. (c) Computed CL path. (d) Concave and convex regions of the design curve. (e) Feasible C-space left after removing global gouging obstacles. (f) Feasible C-space left after removing rear gouging obstacles. (g) Common feasible C-space (intersection of (e) and (f)).

DOFs of the cutter as a single DOF of the parameter — call it t — that represents one C-space dimension. The second DOF of the cutter — its in-plane rotation — forms the second dimension of the C-space. Thus, the full C-space of this problem is a 2-dimensional rectangle whose one dimension is parameter t for the cutter location and the other dimension is the cutter rotation angle θ (ranging from -90° to $+90^\circ$).

However, the actual “feasible” C-space is limited due to various constraints on the problem. Gouging constraints restrict the possible orientations [Jun et al. 2003], while the scallop height limit restricts both orientations and positions of CL points [Lin and Koren 1996].

We compute and subtract obstacles for local, rear, and global gouging [Lasemi et al. 2010] individually from the full C-space. Local gouging occurs when the local radius of curvature is smaller than the cutter radius [Jensen 1993]. Rear gouging occurs when the cutter is inclined such that its back side collides with the curve [Kiswanto et al. 2007], while global gouging occurs when the cutter body collides with the design curve [Wang and Tang 2008]. We perform the following steps to identify the gouging obstacles in our problem:

- We sample the curve to determine candidate CC (Fig. 7.4(a-b)) and corresponding CL points (Fig. 7.4(c)) on the curve. In the optimization phase, we will consider subsets of these computed CL points as the SDC candidates.
- We determine local gouging obstacles by first dividing the design curve into its concave

and convex areas (red and green in Fig. 7.4(d)) and computing the local radius of curvature (r) at each sampled CC point. We check for local gouging ($r < \rho$, the cutter radius) and report that portion of the curve as unmachinable with this tool. Otherwise, there are no C-space obstacles due to local gouging, as is the case for the curve in Fig. 7.4(a).

- We determine rear gouging obstacles at each CC point using local tangents and the tool shadow region — the projection of the cutter on the design curve along the local surface normal. We perform 2D computations following the method for 3D tool shadow region calculations reported by Kiswanto et al. [Kiswanto et al. 2007] to compute rear gouging limits on either side of each CC point. One example of a gouging limit is shown in Fig. 7.3 with angle θ_1 . Fig. 7.4(e) shows the portions of the full C-space remaining after removing the rear gouging obstacles for all CC points for the design curve in Fig. 7.4(a).
- We compute global gouging obstacles by an inverse approach. We use the fact that only convex regions of the design curve can act as collision sites where global gouging could happen. But, instead of searching for collision sites from every CC point, we do an inverse computation of identifying CC points on the design curve corresponding to each collision site (i.e. convex regions of the curve). We construct and use the “visibility chart” of the curve [Elber et al. 2005b] to determine and set limits to the “visible” CC points from every collision site (θ_2 in Fig. 7.3). These limits are updated to the smallest range if the same CC point on the design curve is visible from multiple collision sites. Fig. 7.4(f) shows the portions of the full C-space remaining after removing the global gouging obstacles for all CC points for the design curve in Fig. 7.4(a).

When combined, the final feasible C-space (computed by subtracting both rear and global gouging obstacles) is seen in Fig. 7.4(g). Now, we perform a search for an SDC in this feasible C-space.

Optimal SDC search

We search for an SDC in the feasible C-space with the two objectives of minimizing machining time and maximizing material removal rate (MRR). The first objective of minimizing machining time dictates that the cutter orientations change as little as possible during the process since time is lost in cutter orientation changes. At the same time, MRR is maximized only when the cutter orientation is identical to the local surface normal. These could be contradictory objectives in most freeform surfaces. We must keep varying the orientation as the surface normal varies for maximum MRR, but we must also not vary it “too much” to avoid excessive orientation changes. Further, sometimes inclining the cutter exactly normal to the surface may not be feasible due to global gouging obstacles. Thus, we need an algorithm to plan an SDC while considering conflicting objectives in a possibly discontinuous parameter space. Also, we must ensure that CL points are planned so as to

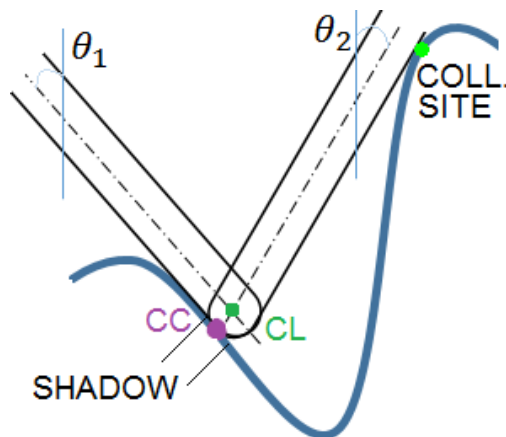


Figure 7.3: Computing rear and global gouging obstacles (orientation limits)

“machine” the design curve completely. As discussed in section 7.3.2, we will first define the mathematical objective function to determine its characteristics in order to choose an appropriate optimization technique. We can combine the two objectives as:

$$\text{Min. } \bar{g} = w_1 \cdot \sum_i (|\theta_{i+1} - \theta_i|) + w_2 \cdot \sum_i (|\theta_i - N_i|) \quad (7.1)$$

where N_i is the orientation of the curve normal at the i th CC point and w_1, w_2 are relative weights assigned to the two objectives of summed angular change ($|\theta_i - \theta_{i-1}|$) and deviation of the cutter orientation from the local surface normal ($|\theta_i - N_i|$).

In the absence of analytical expressions for C-space boundaries and obstacles, and because the feasible C-space may be discontinuous, we cannot use gradient based optimization techniques for this optimization. In addition, deterministic optimization techniques suffer from numerical instability or error accumulation when numerous computations such as numerical integration are repeatedly performed in iterative steps. On the other hand, heuristic optimization techniques such as genetic algorithms (GAs) [Goldberg 1989] may suit our requirements since GAs do not impose many mathematical conditions on the objective function. GAs can be applied to any optimization problem without the need of a differentiable objective function. In addition, parallel versions of GAs are also available to harness the compute power of multi-core CPUs or GPUs [Knysh and Kureichik 2010]. We made following implementation decisions when applying GAs to this problem.

- We define a custom chromosome that allows variable length toolpaths with fixed bits by encoding CL positions into ON/OFF bits such that each chromosome can have a different set of CL points as its SDC. During fitness computation (computing the objective function value for a candidate chromosome), we read and decipher the chromosome and compute its fitness by summing over all CL points that may be turned ON in that chromosome.

- In addition to the gouging constraints on the C-space, we set an additional non-linear constraint during the algorithm run to ensure that every toolpath (chromosome) is valid by restricting the distance between two consecutive CC points (toolpath interval) such that the resulting scallop height never exceeds the limit. We use the following expression from [Loney and Ozsoy 1987, Suresh and Yang 1994] to compute scallop height (h) from step interval (s) and radius of the tool (R):

$$s = 2\sqrt{h(2R - h)}.$$

- We also enforce a constraint such that CL points corresponding to the first and the last CC points on the curve must be present in any SDC candidate. Together with the scallop threshold constraint, this ensures that the complete design curve gets machined.

7.5 Results and discussion

7.5.1 Experimental setup

In order to perform truly global search while avoiding local optima in finite time, GA can be customized based on the problem characteristics by adjusting various algorithm parameters. We used Matlab's implementation of GAs in the optimization toolbox. Based on the recommended problem size to population size relationship for large scale engineering optimization problems in [De Jong and Spears 1991], we performed several calibration experiments to conclude that we needed a population size of 20 times the number of evaluated CC points. The process was less sensitive to other parameter values (we tested for 5%-35% elite population retention, 0.2-0.8 two-point cross-over probability); we retained the default Matlab values of 10% elite population retention, roulette wheel selection strategy, and two point cross-over with 0.6 probability. We set the stopping criterion of weighted average change in fitness function value over stalled generations (iterations with little or no improvement in fitness function value) $1e-6$ for 50 stalled generations. With these parameters, we found that the algorithm converged after approximately 1500-1700 generations and produced repeatable results.

7.5.2 Results: lower dimensional problem

We illustrate two contrasting results in Fig. 7.4 (a) and (b). The green line indicates the surface normal orientation, red and cyan lines indicate the lower and upper bounds on the shaded C-space, and the solution SDC is indicated by a blue line connecting purple dots that indicate CL positions and orientations.

In the first example, Fig. 7.4(a), we set the weights w_1 and w_2 equal, with an intent to find a toolpath that will maximize — as much as possible — the MRR (by inclining the tool closer to the local surface normal), and, at the same time, minimize — as much as possible — frequent orientation changes. Fig. 7.4(a) shows the resulting toolpath, plotted on the feasible C-space. We observe that the toolpath follows the surface normals (green curve)

when they are well within the constraints (inside the shaded region) and avoids sudden orientation changes.

In the second example, Fig. 7.4(b), we set the weight for MRR lower than the weight for orientation change. As seen in the plotted toolpath, the obtained toolpath was significantly different, much “flatter” (indicating fewer orientation changes) and only somewhat influenced by the surface normal curve, but still remaining inside the shaded region.

Thus, depending on the objective of the machinist, the algorithm can generate optimized paths that follow the set constraints while optimizing the particular set of objectives the user intended. This completes the example implementation to solve the lower-dimensional variant of the problem.

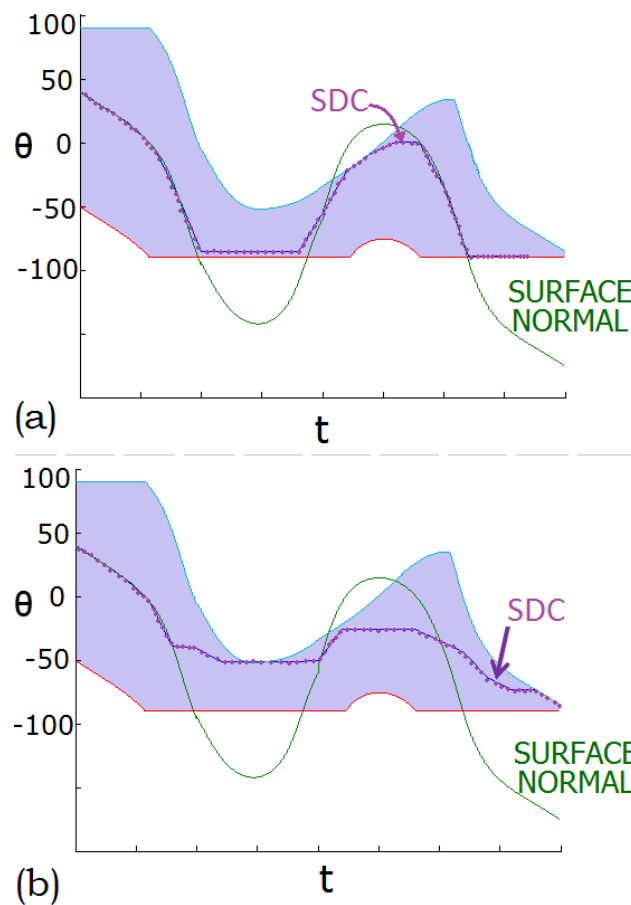


Figure 7.4: Results obtained after optimization (a) With equal weights to machining time and MRR (b) With less importance to MRR and more importance to machining time

7.6 Summary

In this chapter, we have proposed a strategy to formulate the full 5-axis toolpath planning problem by transforming it to a multi-objective non-linear optimization problem in the C-space of the cutter. As we identified in the review of literature, a truly optimal solution to the 5-axis toolpath planning problem necessitates simultaneous solutions of involving sub-problems but none of the existing approaches formulate such a compound problem due to the inherent complexity. Our formulation method considers all DOFs of the cutter simultaneously without making any simplifying assumptions. A 5-axis toolpath planning system based on our formulation may be able to find the optimal toolpath solution in the full C-space of feasible solutions — not possible by existing approaches that limit the search to “slices” of the complete solution space. As a result, our formulation can enable solution to the two sub-problems of cutter locations and cutter orientations simultaneously. We identify characteristics of C-space-appropriate optimization techniques (multi-objective, non-linear optimization in discontinuous multi-dimensional spaces) that can be used when searching for the optimal toolpath. Our formulation offers flexibility for formulating subset problems (by changing the constraints) or for considering additional objectives (by changing the objective function). We illustrate the use of our method with a proof-of-concept implementation for a lower-dimensional problem: an artificial representative problem that facilitates easy visualization of the C-space and obtained solutions.

Reducing energy consumption in CNC machining has been the ultimate goal of this thesis. Work reported in this chapter, in our opinion, is a novel foundation over which, advanced 5-axis toolpath planning systems may be built to obtain toolpaths that minimize several, often conflicting objectives, simultaneously. Unlike the research reported on 3-axis machines in Chapters 3 through 5, that can be readily applied in industrial applications to save energy, the true potential of the work reported in this chapter may be realized when this formulation is augmented with further research to develop a complete 5-axis toolpath planning system.

Chapter 8

Conclusions and Future Work

In this dissertation, we address energy efficiency in manufacturing specific to multi-axis CNC milling machines. To improve energy efficiency, we focus on reducing the energy consumed in machining. We identify and illustrate the inherent differences in energy consumption behaviors of 3- and 5-axis CNC machines and thus treat them differently, to analyze, model, and suggest ways to improve energy consumption behavior. The knowledge, techniques, and software tools developed in this work can be readily used in manufacturing industry at various stages in the manufacturing cycle of a part, to save energy (electricity). The major contributions of this dissertations can be summarized as:

1. We demonstrate that energy consumption is an important, independent parameter to consider when planning CNC manufacturing processes — a view that goes beyond simply associating energy consumption to the cycle (operation) time or MRR alone.
2. For 3-axis CNC machines:
 - (a) We propose an analytical model for energy consumption by 3-axis CNC machines (Chapter 3) and provide evidence based on machining trials that validates the predictions made by the model. The novelty of our energy consumption model is that it predicts energy usage for an NC code without the need of any handbook data or machine specifications, purely based on a one-time customization trial that customizes the model to a new CNC machine.
 - (b) We also report the development of an energy analyzer software tool to compare electrical performance of NC codes (toolpaths) using the proposed energy model. The energy analyzer (described in Chapter 4) estimates machining time and electricity consumption for a provided NC code, when executed on the specified CNC machine. Using the energy estimates for various alternative toolpaths for a component, process planners can determine the most energy efficient toolpath for an operation for a specific CNC machine. To our knowledge, no existing tool can perform such a customized analysis of toolpaths for a specific CNC machine to predict energy consumption requirements.

- (c) We demonstrate test cases indicating up to 20% electricity saving (for the Haas VF-0 machine) using the energy analyzer by comparing and selecting an appropriate toolpath from the available choices obtained using CAM software. We anticipate even larger energy savings for larger CNC machines found on industrial shop floors today.
 - (d) Based on our analyses of numerous NC codes using our energy analyzer, we identify characteristics of 3-axis NC toolpaths that play an important role in energy consumption behavior. The identified characteristics include segment lengths, number of corners, and primary cutting direction.
 - (e) Further, we propose that inherently energy efficient toolpaths can be generated by adhering to the identified characteristics of energy efficient toolpaths. As a proof-of-concept, we show (using actual machining trials as well as energy analyzer estimates) that a toolpath generated based on some of the identified characteristics (inspired from research on digital micrography) consumes less energy when compared with toolpaths generated using commercial CAM software for the same material removal rate.
3. For 5-axis CNC machines:
- (a) We identify that toolpath planning for optimizing machining time holds the key to improve energy efficiency in the case of 5-axis CNC machines. 5-axis toolpath planning consists of CL path planning and tool orientation planning: two sub-problems that must be solved simultaneously for a truly optimal solution. Further, we provide evidence (based on an extensive literature review) that to our knowledge, none of the existing approaches formulate or solve such a simultaneous problem due to the inherent complexity in the parent problem.
 - (b) Our main contribution in this area is a unified formulation of the complete problem that avoids approximations or separations of the inherent 5 DOFs. To our knowledge, no problem formulation reported till date truly considers all 5 DOFs of the problem simultaneously.
 - (c) Our formulation is based on C-space optimization; we also provide procedures to translate the complete 5-axis CNC toolpath planning problem to the proposed C-space based optimization problem.
 - (d) We also demonstrate — for a lower dimensional analogue — a solution process to solve the formulated C-space optimization problem using a multi-dimensional optimization algorithm. Our lower-dimensional implementation is aimed at providing a proof of concept that the proposed formulation strategy can be used to simultaneously solve for rotational and translational DOFs of a problem. We believe that this formulation can be used/further extended to develop a complete 5-axis toolpath planning system that can lead to a more optimal toolpaths that are not possible to obtain with any of the existing approaches.

We identify several future research tasks for 3- and 5-axis CNC machining in the following sections.

8.1 Future work on 3-axis machining

Our work on analyzing, modeling, and estimating energy consumption of 3-axis CNC milling machines is readily applicable in today's industry. Further work in this area will benefit from having the analyzer to quickly compare toolpaths for their energy consumption on any CNC machine using the energy analyzer saving precious resources in machining trials. We propose a few extensions to this research as follows.

- Improving usability and accuracy: As we identified in the limitations, energy analyzer estimates suffer from limitations of the data acquisition process, insistence on not using the machine handbook data, and from the need of equipment that is not available today. A custom designed energy meter which is easy to integrate with and install on a new machine must be developed for this task. Development of MTCConnect standard [Vijayaraghavan et al. 2008] is a promising effort in this direction.
- Energy efficient toolpaths by design: Generating 3-axis toolpaths that are inherently energy efficient seems a plausible extension of this research. We anticipate, based on our proof-of-concept analysis in Chapter 6, that opportunities to save energy right during the toolpath planning stage also exist. If micrography-based toolpaths are generated, methods to automatically design a suitable vector field, trace equally-spaced streamlines, and to connect the streamlines efficiently to form a complete toolpath must be developed.
- Machine specific toolpaths: In addition to inherently energy-efficient toolpaths based on the workpiece geometry, an interesting area of research may be generating machine-specific, energy-efficient toolpaths. Machine customization data can be used as an input in the toolpath generation process to generate such toolpaths. To our knowledge, none of the existing CAM software have the ability to optimize toolpaths for energy consumption and/or for a particular CNC machine.

8.2 Future work on 5-axis machining

It is acknowledged in the research community that finding a truly optimal 5-axis toolpath is still an unsolved problem because none of the existing approaches solve the full 5-DOF problem without making simplifying assumptions or approximations that result in separation of the 5 DOFs of the problem. We believe that the work reported in this dissertation advances the knowledge-front with a *unified* problem formulation and solution strategy that can, in the future, lead to a near-optimal solution for the complete 5-DOF problem without separating

DOFs or making approximations. In developing a 5-axis toolpath planning system based on our formulation, following aspects may require additional research.

- **CL points and connectivity:** In 5-axis machining, a CC point can be machined from several possible CL points due to the 3-dimensional nature of the geometry. As a result, there is no one-to-one correspondence between CL and CC points as there was in the case of the lower-dimensional analogue. Therefore, the feasible C-space of configurations for each CC point is a 5D solid consisting of all possible locations of CL points that can machine the CC point along with possible orientation ranges. Computing and search in such a higher-dimensional space for larger components can be extremely compute intensive. Adaptive sampling strategies discussed in [Nelaturi and Shapiro 2013] can be effectively used here to reduce the computational efforts.
- **Toolpath connectivity:** Multiple strategies to connect CL points are possible in the case of 5-axis CNC toolpaths, e.g. contour parallel, spiral, zig-zag, etc. This is different from the lower-dimensional problem where only one logical order of visiting the CC points (along the parametric direction e.g. left to right) was feasible. Further, depending on the strategy, the same set of CL points may result in a different machining time for the operation. Thus, when optimizing, the connectivity of CL points has to be explicitly considered in the case of true 5-axis toolpaths. This can be achieved in the optimization process by defining the objective function dependent not only on the constituent CL points but also the order in which they appear. Additional constraints may be also required to ensure that the prospective solutions, containing CL points and their connectivity, do in fact result in complete machining of the component.
- **Scallops:** The scallops formed around a CC point when machining a 3D component on a 5-axis CNC machine are affected by both the current and the adjacent CL path. Thus, in many existing 5-axis toolpath planning algorithms, scallops are computed and minimized by first fixing a set of CC points, followed by computing tool orientations at each CC point to maintain or minimize the resulting scallop heights. However, fixing a set of CC points does amount to separation of DOFs that we want to avoid.

As a remedy, when developing a 5-axis toolpath planning system based on our proposed formulation, a basic toolpath topology can be enforced on each candidate solution during the optimization process. The enforced topology can even change between generations of an evolutionary algorithm. Without fixing the coordinates of CL points, such a topology restriction will enable the algorithm to compute scallop heights around any CL point in each solution to ensure it remains under the design constraint. Thus, in essence, toolpath planning can be done iteratively to maintain scallops below a minimum by changing both CL points and orientations simultaneously.

- **Computational complexity:** It is evident that most of the computations in 5-axis machining will be significantly more complex than the lower-dimensional analogue. We propose a two-pronged approach to approach realistic solutions in a reasonable

time-frame. First, we propose sampling the C-space, obstacles, and the boundaries adaptively such that computations are limited. As observed in the lower dimensional analogue, C-space boundaries are continuous where sampling adaptively based on the underlying geometric characteristics results in a reasonable approximation. [Nelaturi and Shapiro 2013] and [Ilushin et al. 2005] propose adaptive sampling strategies for 5-axis machining and obstacle detection that can be used to limit computations. Secondly, most of the proposed computations in our approach are data-parallel and can be performed independently for every CC point on a surface. This makes the approach a suitable candidate for using parallel computational hardware such as the GPUs to speed up the computations. Further, the optimization process can be parallelized too — some examples of such algorithms can be found in [Arenas et al. 2011].

CNC machining encompasses a variety of manufacturing processes including cutting, milling, turning, and grinding. We focused on CNC point-milling in this dissertation but most of the treatment related to analysis and modeling can be readily extended to other CNC manufacturing processes to improve their performance and energy usage. In this dissertation, we proposed and implemented several ideas (specific to CNC process planning) that demonstrated the need for considering energy usage as an independent metrics when designing and comparing manufacturing operations, in addition to the conventionally considered metrics of process productivity and cycle time. With ever-stricter environmental standards requiring tangible progress toward saving energy in industrial operations, the knowledge and the tools developed in this dissertation can be readily used, especially because they do not require any changes to the existing practices or infrastructure. As we move to sustainable manufacturing, we hope that efforts to save energy in manufacturing will benefit from this dissertation research.

Bibliography

- K. Ahmadi and F. Ismail. Machining chatter in flank milling. *International Journal of Machine Tools and Manufacture*, 50(1):75 – 85, 2010.
- Y Altintas. Prediction of cutting forces and tool breakage in milling from feed drive current measurements. *Journal of Engineering for Industry (Transactions of the ASME)*, 114(4): 386–392, 1992.
- Weerachai Anotaipaboon and Stanislav S. Makhanov. Curvilinear space-filling curves for five-axis machining. *Computer-Aided Design*, 40(3):350 – 367, 2008.
- M.G. Arenas, A.M. Mora, G. Romero, and P.A. Castillo. GPU computation in bioinspired algorithms: A review. In *Advances in Computational Intelligence*, volume 6691 of *Lecture Notes in Computer Science*, pages 433–440. Springer Berlin Heidelberg, 2011.
- Oliver Ioan Avram and Paul Xirouchakis. Evaluating the use phase energy requirements of a machine tool system. *Journal of Cleaner Production*, 19(6):699 – 711, 2011.
- Abdullahil Azeem, Hsi-Yung Feng, and Lihui Wang. Simplified and efficient calibration of a mechanistic cutting force model for ball-end milling. *International Journal of Machine Tools and Manufacture*, 44(2):291–298, 2004.
- M. Balasubramaniam, P. Laxmiprasad, S. Sarma, and Z. Shaikh. Generating 5-axis NC roughing paths directly from a tessellated representation. *CAD Computer Aided Design*, 32(4):261–277, 2000.
- Vincent Aizebeoje Balogun and Paul Tarisai Mativenga. Modelling of direct energy requirements in mechanical machining processes. *Journal of Cleaner Production*, 41(0): 179 – 186, 2013.
- Vincent Aizebeoje Balogun, Ampara Aramcharoen, Paul Tarisai Mativenga, and Shaw Kah Chuan. Impact of machine tools on the direct energy and associated carbon emissions for a standardized NC toolpath. In Andrew Y. C. Nee, Bin Song, and Soh-Khim Ong, editors, *Re-engineering Manufacturing for Sustainability*, pages 197–202. Springer Singapore, 2013. ISBN 978-981-4451-47-5.

- M. Barakchi Fard and Hsi-Yung Feng. Effect of tool tilt angle on machining strip width in five-axis flat-end milling of free-form surfaces. *The International Journal of Advanced Manufacturing Technology*, 44:211–222, 2009.
- Thomas Behrendt, Andre Zein, and Sangkee Min. Development of an energy consumption monitoring procedure for machine tools. *CIRP Annals - Manufacturing Technology*, 61(1):43 – 46, 2012.
- MD Bovea and V Pérez-Belis. A taxonomy of ecodesign tools for integrating environmental requirements into the product design process. *Journal of Cleaner Production*, 20(1):61–71, 2012.
- E Budak, Y Altintas, and EJA Armarego. Prediction of milling force coefficients from orthogonal cutting data. *Journal of engineering for industry*, 118(2):216–224, 1996.
- E. Budak, E. Ozturk, and L.T. Tunc. Modeling and simulation of 5-axis milling processes. *CIRP Annals - Manufacturing Technology*, 58(1):347 – 350, 2009.
- Kenneth Castelino, Roshan D’Souza, and Paul K. Wright. Toolpath optimization for minimizing airtime during machining. *Journal of Manufacturing Systems*, 22(3):173 – 180, 2003.
- Hsin-Pao Chen, Hsin-Hung Kuo, and Der-Min Tsay. Removing tool marks of blade surfaces by smoothing five-axis point milling cutter paths. *Journal of Materials Processing Technology*, 209(17):5810 – 5817, 2009.
- Y.D. Chen, J. Ni, and S. M. Wu. Real-time CNC tool path generation for machining iges surfaces. *Journal of engineering for industry*, 115(4):480–486, 1993.
- Chuang-Jang Chiou and Yuan-Shin Lee. A machining potential field approach to tool path generation for multi-axis sculptured surface machining. *Computer-Aided Design*, 34(5): 357 – 371, 2002.
- B.K. Choi, D.H. Kim, and R.B. Jerard. C-space approach to tool-path generation for die and mould machining. *CAD Computer Aided Design*, 29(9):657–669, 1997.
- S. Choi, D. Kong, S. Park, S. Pavanaskar, and Y. Yasui. Evaluation of tool-path w.r.t. precision and environment. Technical report, University of California, Berkeley, 2009. Project report for E290C class, Fall 2009.
- CNC Cookbook. Cnc cookbook. <http://www.cnccookbook.com/CCNCMillFeedsSpeedsClimbConventional.htm>, 2014.
- Continental Control Systems. Wattnode pulse meter. http://www.ccontrols.com/WattNode_Pulse, 2009-2014.

- Inc. Dassault Systems. *Solidworks 2013*. Concord, Massachusetts, 2013. URL <http://www.solidworks.com/>.
- Kenneth A De Jong and William M Spears. An analysis of the interacting roles of population size and crossover in genetic algorithms. In *Parallel problem solving from nature*, pages 38–47. Springer, 1991.
- Nancy Diaz, Elena Redelsheimer, and David Dornfeld. Energy consumption characterization and reduction strategies for milling machine tool use. In JÄijrgen Hesselbach and Christoph Herrmann, editors, *Glocalized Solutions for Sustainability in Manufacturing*, pages 263–267. Springer Berlin Heidelberg, 2011.
- D Dragomatz and S Mann. A classified bibliography of literature on NC milling path generation. *Computer-Aided Design*, 29(3):239 – 247, 1997.
- JR Duflou, Karel Kellens, and Wim Dewulf. Unit process impact assessment for discrete part manufacturing: A state of the art. *CIRP Journal of Manufacturing Science and Technology*, 4(2):129–135, 2011.
- Gershon Elber and Elaine Cohen. Toolpath generation for freeform surface models. *Computer-Aided Design*, 26(6):490 – 496, 1994.
- Gershon Elber, Elaine Cohen, and Sam Drake. MATHSM: medial axis transform toward high speed machining of pockets. *Computer-Aided Design*, 37(2):241–250, 2005a.
- Gershon Elber, Robert Sayegh, and Gill Barequet. Two-dimensional visibility charts for continuous curves. In *Shape Modeling and Applications, 2005 International Conference*, pages 206–215. IEEE, 2005b.
- Rida T. Farouki and Shiqiao Li. Optimal tool orientation control for 5-axis CNC milling with ball-end cutters. *Computer Aided Geometric Design*, 30(2):226 – 239, 2013.
- Rida T. Farouki, Chang Yong Han, and Shiqiao Li. Inverse kinematics for optimal tool orientation control in 5-axis CNC machining. *Computer Aided Geometric Design*, 30(3), 2013.
- Hsi-Yung Feng and Chia-Hsiang Menq. The prediction of cutting forces in the ball-end milling process—Äi. model formulation and model building procedure. *International Journal of Machine Tools and Manufacture*, 34(5):697 – 710, 1994. ISSN 0890-6955.
- Hsi-Yung Feng and Zhengji Teng. Iso-planar piecewise linear NC tool path generation from discrete measured data points. *Computer-Aided Design*, 37(1):55–64, 2005.
- V. Giri, D. Bezbaruah, P. Bubna, and A. Roy Choudhury. Selection of master cutter paths in sculptured surface machining by employing curvature principle. *International Journal of Machine Tools and Manufacture*, 45(10):1202 – 1209, 2005.

- David E. Goldberg. *Genetic Algorithms in search optimization and machine learning*. Addison-Wesley Publishing, 1989.
- Hu Gong, F.Z. Fang, X.T. Hu, Li-Xin Cao, and Jian Liu. Optimization of tool positions locally based on the BCELTP for 5-axis machining of free-form surfaces. *Computer-Aided Design*, 42(6):558 – 570, 2010.
- Google Inc. Google ChartsAPI. <http://code.google.com/intl/en/apis/chart/>, 2010-2014.
- P. Gray, S. Bedi, and F. Ismail. Rolling ball method for 5-axis surface machining. *Computer-Aided Design*, 35(4):347 – 357, 2003.
- Paul J. Gray, Sanjeev Bedi, and Fathy Ismail. Arc-intersect method for 5-axis tool positioning. *Computer-Aided Design*, 37(7):663 – 674, 2005.
- Paul J. Gray, Fathy Ismail, and Sanjeev Bedi. Arc-intersect method for 3-axis tool paths on a 5-axis machine. *International Journal of Machine Tools and Manufacture*, 47(1):182 – 190, 2007.
- Timothy Gutowski, Cynthia F Murphy, David T Allen, Diana J Bauer, Bert Bras, Thomas S Piwonka, Paul S Sheng, John W Sutherland, Deborah L Thurston, and Egon E Wolff. Environmentally benign manufacturing. *Baltimore, MD, International Technology Research Institute, World Technology WTEC Division*, 2001.
- Timothy Gutowski, Cynthia Murphy, David Allen, Diana Bauer, Bert Bras, Thomas Piwonka, Paul Sheng, John Sutherland, Deborah Thurston, and Egon Wolff. Environmentally benign manufacturing: observations from japan, europe and the united states. *Journal of Cleaner Production*, 13(1):1–17, 2005.
- Timothy Gutowski, Jeffrey Dahmus, and Alex Thiriez. Electrical energy requirements for manufacturing processes. In *13th CIRP international conference on life cycle engineering, Leuven, Belgium*, volume 5, pages 560–564, 2006.
- Z. Han and D. C. H. Yang. Iso-phote based tool-path generation for machining free-form surfaces. *Journal of Manufacturing Science and Engineering, Transactions of the ASME*, 121(4):656–664, 1999.
- Z. Han, D. C. H. Yang, and J. J. Chuang. Isophote-based ruled surface approximation of free-form surfaces and its application in NC machining. *International Journal of Production Research*, 39(9):1911–1930, 2001.
- Y He, F Liu, T Wu, FP Zhong, and B Peng. Analysis and estimation of energy consumption for numerical control machining. *Proceedings of the Institution of Mechanical Engineers, Part B: Journal of Engineering Manufacture*, 226(2):255–266, 2012.

- M Held, G Lukacs, and L Andor. Pocket machining based on contour-parallel tool paths generated by means of proximity maps. *Computer-Aided Design*, 26(3):189 – 203, 1994.
- Timothy Herzog. World greenhouse gas emissions. *WRI working paper in World Resources Institute*, 2005.
- Ming-Che Ho, Yean-Ren Hwang, and Chang-Hsia Hu. Five-axis tool orientation smoothing using quaternion interpolation algorithm. *International Journal of Machine Tools and Manufacture*, 43(12):1259 – 1267, 2003.
- Oleg Ilushin, Gershon Elber, Dan Halperin, Ron Wein, and Myung-Soo Kim. Precise global collision detection in multi-axis NC-machining. *Computer-Aided Design*, 37(9):909 – 920, 2005.
- C. G. Jensen. *Analysis and synthesis of multi-axis sculptured surface machining*. PhD thesis, Purdue University, 1993.
- C. G. Jensen and D. C. Anderson. A review of numerically controlled methods for finish-sculptured-surface machining. *IIE Transactions*, 28(1):30–39, 1996.
- Cha-Soo Jun, Kyungduck Cha, and Yuan-Shin Lee. Optimizing tool orientations for 5-axis machining by configuration-space search method. *Computer-Aided Design*, 35(6):549 – 566, 2003.
- S Kara and W Li. Unit process energy consumption models for material removal processes. *CIRP Annals-Manufacturing Technology*, 60(1):37–40, 2011.
- Petra Kersting and Andreas Zabel. Optimizing NC-tool paths for simultaneous five-axis milling based on multi-population multi-objective evolutionary algorithms. *Advances in Engineering Software*, 40(6):452 – 463, 2009.
- G. Kiswanto, B. Lauwers, and J.-P. Kruth. Gouging elimination through tool lifting in tool path generation for five-axis milling based on faceted models. *International Journal of Advanced Manufacturing Technology*, 32(3-4):293–309, 2007.
- D.S. Knysh and V.M. Kureichik. Parallel genetic algorithms: a survey and problem state of the art. *Journal of Computer and Systems Sciences International*, 49(4):579–589, 2010.
- D. Kordonowy. A power assessment of machining tools. Master’s thesis, Massachusetts Institute of Technology, Cambridge, MA, USA, 2002.
- Ali Lasemi, Deyi Xue, and Peihua Gu. Recent development in CNC machining of freeform surfaces: A state-of-the-art review. *Computer-Aided Design*, 42(7):641 – 654, 2010.

- Ritwik Layek, Hazem Nounou, Mohamed Nounou, Aniruddha Datta, and Shankar P Bhattacharyya. A measurement based approach for linear circuit modeling and design. In *Decision and Control (CDC), 2012 IEEE 51st Annual Conference on*, pages 3821–3826. IEEE, 2012.
- H. Li and H.-Y. Feng. Efficient five-axis machining of free-form surfaces with constant scallop height tool paths. *International Journal of Production Research*, 42(12):2403 – 2417, 2004.
- Huiwen Li, O. Tutunea-Fatan, and Hsi-Yung Feng. An improved tool path discretization method for five-axis sculptured surface machining. *The International Journal of Advanced Manufacturing Technology*, 33:994–1000(7), 2007. doi: doi:10.1007/s00170-006-0529-z.
- Rong-Shine Lin and Y. Koren. Efficient tool-path planning for machining free-form surfaces. *Journal of Engineering for Industry*, 118(1):20–28, 1996.
- Chih-Ching Lo. Efficient cutter-path planning for five-axis surface machining with a flat-end cutter. *Computer-Aided Design*, 31(9):557–566, 1999.
- Gregory C Loney and Tulga M Ozsoy. NC machining of free form surfaces. *Computer-Aided Design*, 19(2):85 – 90, 1987.
- Tomas Lozano-Perez. Spatial planning: A configuration space approach. *Computers, IEEE Transactions on*, 100(2):108–120, 1983.
- J Lu, R Cheatham, CG Jensen, Y Chen, and B Bowman. A three-dimensional configuration-space method for 5-axis tessellated surface machining. *International Journal of Computer Integrated Manufacturing*, 21(5):550–568, 2008.
- R. Maharik, M. Bessmeltsev, A. Sheffer, A. Shamir, and N. Carr. Digital micrography. *Transactions on Graphics (Proc. SIGGRAPH 2011)*, pages 100:1–100:12, 2011.
- S.S. Makhanov. Space-filling curves in adaptive curvilinear coordinates for computer numerically controlled five-axis machining. *Mathematics and Computers in Simulation*, 79(8):2385 – 2402, 2009.
- S. Marshall and J.G. Griffiths. A new cutter-path topology for milling machines. *Computer-Aided Design*, 26(3):204 – 214, 1994.
- ME Martellotti. An analysis of the milling process. *Transactions of ASME*, 63:677–700, 1941.
- M Eugene Merchant. Basic mechanics of the metal cutting process. *Journal of Applied Mechanics*, 11(A):168–175, 1944.

- Debananda Misra, V Sundararajan, and Paul K Wright. Zig-zag tool path generation for sculptured surface. In *Geometric and Algorithmic Aspects of Computer-aided Design and Manufacturing: Dimacs Workshop Computer Aided Design and Manufacturing, October 7-9, 2003, Piscataway, New Jersey*, volume 67, page 265. AMS Bookstore, 2005.
- Varinder Kumar Mittal and Kuldip Singh Sangwan. Development of a model of barriers to environmentally conscious manufacturing implementation. *International Journal of Production Research*, 1(1):1–11, 2013.
- M. Mori, M. Fujishima, Y. Inamasu, and Y. Oda. A study on energy efficiency improvement for machine tools. *CIRP Annals - Manufacturing Technology*, 60(1):145 – 148, 2011.
- K. Morishige, K. Kase, and Y. Takeuchi. Collision-free tool path generation using 2-dimensional c-space for 5-axis control machining. *International Journal of Advanced Manufacturing Technology*, 13(6):393–400, 1997.
- Saigopal Nelaturi and Vadim Shapiro. Solving inverse configuration space problems by adaptive sampling. *Computer-Aided Design*, 45(2):373 – 382, 2013.
- S.T. Newman, A. Nassehi, R. Imani-Asrai, and V. Dhokia. Energy efficient process planning for CNC machining. *CIRP Journal of Manufacturing Science and Technology*, 5(2):127 – 136, 2012.
- S. Pande, Z. Hu, K. Ninomiya, and E. Dong. Evaluation of tool-path w.r.t. precision and environment. Technical report, University of California, Berkeley, 2013. Project report for ME220 class, Fall 2013.
- Jianxin Pi, Edward Red, and Greg Jensen. Grind-free tool path generation for five-axis surface machining. *Computer Integrated Manufacturing Systems*, 11(4):337 – 350, 1998.
- Matthieu Rauch, Emmanuel Duc, and Jean-Yves Hascoet. Improving trochoidal tool paths generation and implementation using process constraints modelling. *International Journal of Machine Tools and Manufacture*, 49(5):375 – 383, 2009.
- R. Sarma and D. Dutta. An integrated system for NC machining of multi-patch surfaces. *CAD Computer Aided Design*, 29(11):741–749, 1997.
- S Smith and J Tlusty. An overview of modeling and simulation of the milling process. *Journal of Engineering for Industry (Transactions of the ASME)*, 113(2):169–175, 1991.
- W. Sun, C. Bradley, Y.F. Zhang, and H.T. Loh. Cloud data modelling employing a unified, non-redundant triangular mesh. *CAD Computer Aided Design*, 33(2):183–193, 2001.
- K. Suresh and D. C. H. Yang. Constant scallop-height machining of free-form surfaces. *Journal of Engineering for Industry*, 116(2):253–259, 1994.

- J. Tlustý and F. Ismail. Basic non-linearity in machining chatter. *CIRP Annals - Manufacturing Technology*, 30(1):299 – 304, 1981.
- Stephen Albert Tobias. *Machine-tool vibration*. J. Wiley, 1965.
- S. Tonissen. Power consumption of precision machine tools under varied cutting conditions. Master's thesis, RWTH Aachen, Aachen, Germany, 2009.
- Edward M. Trent and Paul K. Wright. Chapter 2 - metal cutting operations and terminology. In Edward M. Trent and Paul K. Wright, editors, *Metal Cutting*, pages 9 – 20. Butterworth-Heinemann, Woburn, fourth edition, 2000.
- U. S. Energy Information Admin. Annual Energy Review, Rep. DOE/EIA-0384(2008), 2008. URL <http://www.eia.doe.gov/emeu/aer/consump.html>. [Online; accessed 19-July-2008].
- Erkan Ulker, Mehmet Emin Turanalp, and H. Selcuk Halkaci. An artificial immune system approach to CNC tool path generation. *Journal of Intelligent Manufacturing*, 20:67–77, 2009.
- John T Usher. *The modern machinist: a practical treatise on modern machine shop methods*. NW Henley, 1896.
- Dharmaraj Veeramani and Yuh-Shying Gau. Issues in patch-by-patch machining of compound sculptured surfaces. *IIE Transactions*, 30:341–355, 1998.
- Athulan Vijayaraghavan and David Dornfeld. Automated energy monitoring of machine tools. *CIRP Annals-Manufacturing Technology*, 59(1):21–24, 2010.
- Athulan Vijayaraghavan, Will Sobel, Armando Fox, David Dornfeld, and Paul Warndorf. Improving machine tool interoperability using standardized interface protocols: Mt connect. *Info: Green Manufacturing Group, Laboratory for Manufacturing and Sustainability, UC Berkeley*, 2008.
- Nan Wang and Kai Tang. Automatic generation of gouge-free and angular-velocity-compliant five-axis toolpath. *Computer-Aided Design*, 39(10):841 – 852, 2007.
- Nan Wang and Kai Tang. Five-axis tool path generation for a flat-end tool based on iso-conic partitioning. *Computer-Aided Design*, 40(12):1067 – 1079, 2008.
- James P Womack, Daniel T Jones, and Daniel Roos. *The machine that changed the world: The story of lean production—Toyota's secret weapon in the global car wars that is now revolutionizing world industry*. Simon and Schuster, 2007.
- Country Profiles by World Nuclear Association. Nuclear power in China. <http://www.world-nuclear.org/info/Country-Profiles/Countries-A-F/China--Nuclear-Power/>, 2013. [Online; accessed 17-November-2013].

-
- Minyang Yang and Heeduck Park. The prediction of cutting force in ball-end milling. *International Journal of Machine Tools and Manufacture*, 31(1):45 – 54, 1991.
- T. Ye and C.-H. Xiong. Geometric parameter optimization in multi-axis machining. *CAD Computer Aided Design*, 40(8):879–890, 2008.
- W-S Yun and D-W Cho. An improved method for the determination of 3D cutting force coefficients and runout parameters in end milling. *The International Journal of Advanced Manufacturing Technology*, 16(12):851–858, 2000.